European Journal of Medicinal Chemistry 292 (2025) 117668

Contents lists available at ScienceDirect

European Journal of Medicinal Chemistry

journal homepage: www.elsevier.com/locate/ejmech

Review article

Molecular and supramolecular routes to enhance Gadolinium-based contrast agents relaxivity: *How far are we from the theoretical optimal value?*

Lorenzo Palagi [a], Dario Livio Longo [b], Éva Tóth [c], Carlo C. Quattrocchi [d], Aart J. van der Molen [e], Silvio Aime [f], Eliana Gianolio [a,*]

[a] Department of Molecular Biotechnologies and Health Science, Molecular Imaging Center, University of Turin, Turin, Italy
[b] Institute of Biostructures and Bioimaging (IBB), National Research Council of Italy (CNR), Turin, Italy
[c] Centre for Molecular Biophysics, CNRS UPR4301, rue Charles Sadron, 45071, Orléans, France
[d] Centre for Medical Sciences - CISMed, University of Trento, Trento, Italy
[e] Department of Radiology, Leiden University Medical Center, Leiden, the Netherlands
[f] IRCCS SDN SynLab, Naples, Italy

ARTICLE INFO

Keywords:
GBCAs
Gadolinium
contrast media
Magnetic resonance imaging
MRI
relaxivity
Relaxation enhancement

ABSTRACT

Gadolinium Based Contrast Agents (GBCAs) are routinely used in the clinical practice to enhance the diagnostic potential of MRI. Their contrast enhancing capabilities rely on their ability to increase the relaxation rate of tissue water protons. This property is expressed by the relaxivity, whose value is determined by structural, electronic and dynamic characteristics of the GBCA. Based on extensive experimental work over the past four decades and the well-established theory of paramagnetic relaxation, it is usually possible to correlate observed relaxivity values to specific molecular properties. Key determinants include the number of water molecules and/or exchangeable protons in the first and second coordination spheres, their distance from the paramagnetic Gd^{3+} ion, the ion's electronic relaxation time, molecular reorientation time, and the exchange rate of the coordinated water molecules. Understanding the key factors that affect relaxivity has enabled the design of systems with optimized structural and dynamic properties. However, some examples demonstrate exceptional relaxivity which cannot be fully explained by the established theory. In particular, GBCAs within confined environments show significant promise for developing high-relaxivity agents. Overall, one may state that nowadays it is possible to attain highly efficient GBCAs thanks to the in-depth understanding of the structural and dynamic determinants of their relaxivity, together with the optimization of their *in vivo* stability and biodistribution/excretion properties. This knowledge is crucial for the rational design of the next generation of MRI CAs. The domain of Molecular Imaging will also largely benefit from these efforts.

1. Introduction

The contrast observed in an MRI image results from an interplay of multiple factors, including the relative T_1 and T_2 relaxation times of water proton nuclei, tissue proton density, and instrumental settings. MRI's exceptional ability to distinguish between soft tissues has established it as one of the leading imaging techniques for medical diagnostics [1].

Contrast in MRI can be further enhanced through the use of contrast agents (CAs). These paramagnetic compounds significantly accelerate the relaxation rates of water protons, providing not only anatomical detail but also valuable physiological insights. Consequently, the use of CAs has become an integral part of diagnostic protocols, particularly in applications such as organ perfusion assessment, blood-brain barrier evaluation, kidney function analysis, angiography, and tumor detection.

Unlike the contrast agents used in X-ray CT or nuclear medicine, MRI contrast agents do not appear directly in the images. Instead, their presence is inferred from the changes they induce in water proton relaxation rates, which ultimately influence the intensity of the NMR signal [2,3]. Typically, the goal is to shorten T_1 to generate a strong signal within a shorter acquisition time, thereby enhancing the signal-to-noise ratio. Contrast agents that predominantly reduce T_1 are

* Corresponding author. Molecular Imaging Center and Department of Molecular Biotechnologies and Health Science, University of Turin, Via Nizza 52, I-10126, Turin, Italy.
E-mail address: eliana.gianolio@unito.it (E. Gianolio).

https://doi.org/10.1016/j.ejmech.2025.117668
Received 21 March 2025; Received in revised form 18 April 2025; Accepted 19 April 2025
Available online 24 April 2025

classified as positive, whereas those that primarily affect T_2 are termed negative. The search for effective positive CAs has focused on paramagnetic metal complexes, due to the ability of their unpaired electrons to decrease both T_1 and T_2. Among these, Gadolinium-Based Contrast Agents (GBCAs) have emerged as the most effective and widely utilized, with all MRI contrast agents currently in clinical use being Gd-complexes [3–5].

The ability of GBCAs to enhance T_1 contrast in targeted regions depends on both extrinsic and intrinsic factors. Extrinsic factors include the strength of the magnetic field and the used acquisition sequence, while intrinsic properties relate to the specific structure and dynamic behavior of each GBCA, which collectively define its T_1 relaxivity (r_1).

While optimizing the relaxivity of contrast agents is key to improving their efficiency, ensuring high safety standards is equally critical for potential clinical applications.

Increasing attention has been given in recent years to GBCAs long-term safety profile, particularly concerning gadolinium-induced nephrogenic systemic fibrosis (NSF) and the potential for gadolinium deposition in tissues. NSF is a rare but serious condition that was first linked to certain GBCAs in patients with impaired renal function, particularly those based on linear ligands with lower kinetic stability [6]. This led to regulatory restrictions and prompted a shift toward macrocyclic complexes, which offer significantly greater thermodynamic stability and kinetic inertness [7–10], thereby reducing the risk of Gd^{3+} release. More recently, evidence of gadolinium retention in the brain and other tissues, even in individuals with normal renal function, has further underscored the importance of designing agents with minimal dissociation risk and efficient clearance [11,12]. Although no definitive clinical consequences have been demonstrated from Gd deposition at the administered doses of current GBCAs, these findings have reinforced the drive toward developing high-relaxivity agents that can be administered at lower doses. As a result, safety considerations now play a central role in the development of next-generation MRI contrast agents, where efficiency, coordination chemistry, stability, biodistribution, and excretion profiles must be evaluated in an integrated manner as interconnected design parameters.

For all these reasons, this review is not limited to, but primarily focuses on macrocyclic complexes, which are known for their superior thermodynamic stability and kinetic inertness.

2. Results and discussion

2.1. What are the highest theoretically achievable relaxivity values according to paramagnetic relaxation theory?

Relaxivity (r_1) measures the increase in the longitudinal relaxation rate of water protons in solutions containing a paramagnetic metal at the concentration of 1 mM. Over the past three decades, substantial advancements have been made in elucidating the intricate relationships between the structural and dynamic properties of paramagnetic complexes and their relaxivity [4,5]. The observed proton longitudinal relaxation rate (R_{1obs}) in an aqueous solution of a paramagnetic complex is given by the sum of the following terms[3].

i) The diamagnetic contribution (R_1^0), accounting for the relaxation rate of solvent water protons that would have been measured in the presence of a corresponding diamagnetic complex.
ii) The paramagnetic contribution from the exchanging protons in the inner coordination sphere of the metal ion (R_{1p}^{IS}), i.e. coordinated water molecules and/or other mobile protons belonging to ligand's functionalities involved in the coordination scheme of the paramagnetic metal ion. The exchange of these protons with the "bulk" water extends the paramagnetic effect to surrounding solvent water protons.
iii) The paramagnetic contribution from the outer coordination sphere (R_{1p}^{OS}), resulting from interactions between the paramagnetic center and freely diffusing water molecules in its immediate environment.

$$R_{1p}^{obs} = R_1^o + R_{1p}^{IS} + R_{1p}^{OS} \quad (1)$$

Occasionally, a fourth paramagnetic contribution is often considered, arising from mobile protons or water molecules associated to the surface of the chelate in the metal ion second coordination sphere (R_{1p}^{SS}) [13].

The inner-sphere contribution R_{1p}^{IS} is given by:

$$R_{1p}^{IS} = \frac{q[C]}{55.5(T_{1M} + \tau_m)} \quad (2)$$

where [C] is the concentration of the paramagnetic agent, q is the number of water molecules (generally 1 or 2) directly coordinated to the metal ion, τ_m is their exchange lifetime and T_{1M} is the longitudinal relaxation time of the exchanging protons.

T_{1M} is typically assessed using the formula originally derived by Solomon, Bloembergen, and Morgan for simple aqua-ions [14–16]:

$$\frac{1}{T_{1M}} = \frac{2}{15}\left(\frac{\mu_o}{4\pi}\right)^2 \frac{\gamma_I^2 g_e^2 \mu_B^2 S(S+1)}{r_H^6}\left(\frac{7\tau_c}{1+\omega_S^2\tau_c^2} + \frac{3\tau_c}{1+\omega_I^2\tau_c^2}\right) \quad (3)$$

Here, S represents the electron spin quantum number, γ_I denotes the proton nuclear gyromagnetic ratio, while g_e and μ_β correspond to the electronic g factor and the Bohr magneton, respectively. Additionally, ω_I and ω_S refer to the proton and electron Larmor frequencies, respectively, and τ_c represents the correlation time.

τ_c is given by the sum:

$$\tau_c^{-1} = \tau_R^{-1} + \tau_m^{-1} + \tau_s^{-1} \quad (4)$$

Therefore, among the three correlation times—τ_r (reorientational), τ_s (electronic), and τ_m (exchange)—the shortest one dictates the value of τ_C, which consequently determines T_{1M} and, in turn, the overall inner-sphere relaxivity. An analogous treatment holds for R_{1p}^{SS}.

The first generation of commercial contrast agents (CAs) consisted of monohydrated ($q = 1$) complexes with molecular weights ranging from approximately 600 to 800 Da, endowed with rotational correlation times (τ_r) of about 60–80 ps. In this class of complexes, the coordinated water molecule's exchange lifetime (τ_m) typically falls between 200 and 500 ns, while the electronic relaxation time (T_{1e}) is around 1 ns at 0.5 T. These factors contribute to an inner-sphere relaxivity (r_1^{IS}) of roughly 2.5–3.5 $mM^{-1}s^{-1}$ at 25 °C. Under these conditions, it was soon recognized that at 0.5 T, the overall correlation time (τc) is primarily determined by the reorientational correlation time, with a limited influence from both water exchange dynamics and electronic relaxation. According to paramagnetic relaxation theory, relaxivity is maximized when the correlation time (τc) is approximately the inverse of the proton Larmor frequency. By the late 1990s [17], it was understood that the simultaneous optimization of all key parameters could theoretically lead to significantly higher relaxivity values at clinically relevant magnetic field strengths. Specifically, a monohydrated Gd-based probe could achieve T_1 relaxivity values of approximately 100 $mM^{-1}s^{-1}$ at 0.5 T and 60 $mM^{-1}s^{-1}$ at 1.5 T.

Along with correlation times associated with solution dynamics, a critical structural factor affecting inner-sphere relaxivity is the hydration number (q), which acts as a linear scaling factor in Equation (2). An increased number of coordinated water molecules ($q > 1$) provides a distinct benefit for inner-sphere relaxivity, with the value being doubled for Gd-complexes where $q = 2$.

Finally, in some cases, an additional contribution to relaxivity can be obtained when water molecules or exchangeable protons are present in the second coordination sphere of the complex. Although not directly coordinated to the Gd(III) ion, they are held nearby through a network of hydrogen bonds at the ligand's surface, thereby enhancing the observed relaxivity.

2.1.1. How far have we advanced in optimizing molecular tumbling (τ_r) and inner-sphere water exchange (τ_M)?

As anticipated in the previous paragraph, for polyaminocarboxylate complexes of the Gd(III) ion, high relaxivities at imaging fields (0.5–1.5 T) can be achieved when long τr values are present [17]. Consequently, systems with slower motion have been developed to attain high relaxivities. A slowdown of the reorientational dynamics can be achieved by increasing the size of the system as, for spherical molecules, τ_r is proportional to the radius (a) of the molecule as described by the following equation:

$$\tau_R = \frac{4\pi a^3 \eta}{3kT} \quad (5)$$

Basically, three routes have been explored to endow the Gd-chelates with long molecular reorientational times: i) increasing the molecular weight of the metal complex through the introduction of bulky substituents on the ligand structure; ii) forming a covalent or non-covalent adduct between the complex and a slowly tumbling macromolecule (i.e. proteins); iii) designing nanosized supramolecular systems bearing gadolinium(III)-based compounds.

In all cases, the overall rigidity of the system remains a key parameter to achieve high relaxivities. Indeed, fast local motions of the Gd(III) containing units should be prevented in order to take full advantage of the slow rotational dynamics of the entire macromolecule. Internal flexibility was shown to be detrimental for the relaxivity gain in various nanosized paramagnetic probes, including dendrimers [18], polymers [19], micelles [20], etc. This internal flexibility could be quantified via the analysis of ^{1}H relaxation data by separating local and global motions using the Lipari-Szabo formalism, which proved to be useful for the rational design of improved, more rigid paramagnetic systems.

2.1.1.1. – Larger molecular probes. Indeed, this route has been recently exploited in the design of two systems of the "second-generation" GBCAs, namely **Gadopiclenol** (Elucirem®, Guerbet; Vueway®, Bracco) [21], already approved for clinical use, and **Gadoquatrane** (Bayer Healthcare) [22], a tetrameric macrocyclic structure still in clinical trial development, both endowed with increased molecular weight and characterized by relaxivity values that are two-threefold higher than those shown by the "first-generation" GBCAs (Fig. 1) [23]. In the case of Gadopiclenol, the enhanced relaxivity has to be ascribed, apart from the increased molecular weight, to a higher inner sphere hydration ($q = 2$, further discussed in paragraph 1.2) as well as to an additional second sphere contribution [24].

Numerous preclinical studies dealt with molecular probes endowed with increased molecular weight, achieved by either attaching larger side chains to low-molecular-weight Gd-chelates or via assembling multimeric Gd-complexes. Notable examples of the first approach include P846 [25] and P792 [26] that were reported years ago. P846 is a medium-sized, macrocyclic chelate featuring a three-armed structure with a single Gd(III) complex at its core. It has a molecular weight of 3.5 kDa and a hydrodynamic diameter of approximately 4 nm, making it nearly six times larger than Gd-DOTA (0.6 kDa). This increased molecular size leads to significantly enhanced r_1 relaxivity values, reaching 32 $mM^{-1}s^{-1}$ at 1.5 T and 24 $mM^{-1}s^{-1}$ at 3 T (both measured at 37 °C), which are considerably higher than those of conventional low-molecular-weight Gd-DOTA.

P792, also known as Gadomelitol or Vistarem, is a monomeric Gd-DOTA chelate featuring four bulky hydrophilic groups surrounding its core. It has a molecular weight of approximately 6.5 kDa and a hydrodynamic diameter of about 7 nm. This structural arrangement yielded relaxivity values of 27 $mM^{-1}s^{-1}$ at 1.5 T and 12 $mM^{-1}s^{-1}$ at 3 T (both measured at 37 °C). In systems like P846 and P792, a key factor contributing to the enhanced relaxivity appears to be the preferential alignment of the rotation axis along the Gd-H2O vector.

However, the relaxivity drops by more than half when passing from 1.5 T to 3 T, a behavior attributed to the large size of P792. As discussed in session 2, increasing the size of a probe too much can be detrimental for applications at higher field strengths [27].

Among the multimeric Gd-chelates, EP2104R stands out as the only molecular imaging GBCA to have advanced to clinical trials. This fibrin-targeting, tetrameric Gd-based contrast agent is designed for thrombus detection and consists of an 11-amino acid peptide modified with two GdDOTA-like units at both its C- and N-termini, incorporating a total of four Gd ions. When bound to fibrin, EP2104R exhibits a relaxivity of 71.4 $mM^{-1}s^{-1}$ per molecule (equivalent to 17.4 $mM^{-1}s^{-1}$ per Gd) at 37 °C and 1.4 T [28].

In the class of multimeric Gd-chelates several other systems have been proposed, some examples are discussed in section 2.

2.1.1.2. – Adducts with proteins. Since the development of new contrast agents is primarily motivated by the goal of their *in vivo* use, and possible clinical translation, one of the most widely pursued strategies to achieve large-sized systems has been to leverage interactions with endogenous proteins. Since all approved GBCAs are administered *in vivo* through intravenous injection, this approach often looked at the exploitation of human serum albumin (HSA) as the interacting protein (Fig. 2A). In addition to achieving high relaxivities, a strong binding affinity to HSA allows the Gd(III) chelate to remain in the bloodstream for an extended period of time, a key characteristic for an effective blood pool contrast agent in MR angiography.

In this regard, considerable research efforts have been focused on designing Gd(III) chelates with functional groups on their surface that

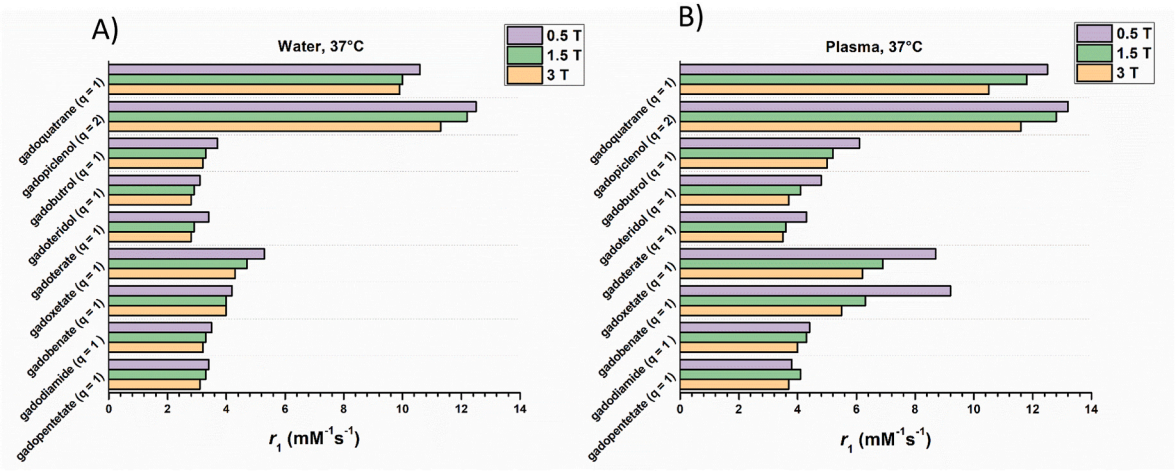

Fig. 1. Longitudinal proton relaxivities (mM−1 s−1) of commercial GBCAs at different magnetic fields, in water (A) and human plasma (B) at 37 °C [21–23].

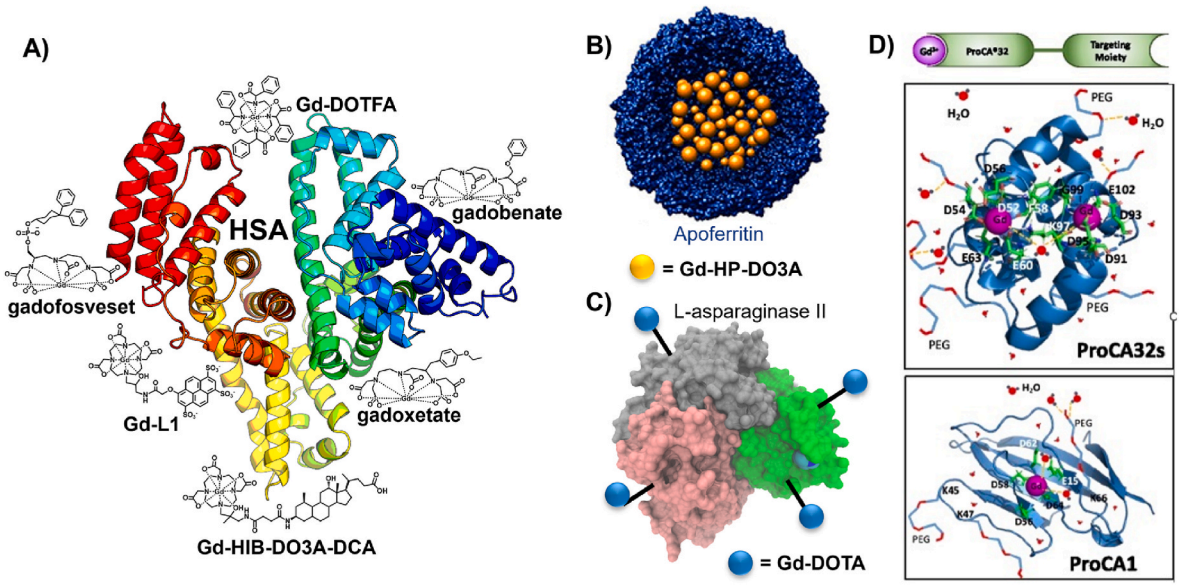

Fig. 2. Examples of slowly tumbling Gd-containing systems based on proteins. Images reported in D) were reproduced with permissions from ref. [52].

facilitate reversible binding to HSA. Early representative examples of such Gd(III) complexes still in clinical use are **Gadoxetate** and **Gadobenate.** They show a relatively weak interaction with serum albumin (K_a = 490 M^{-1} and 250 M^{-1}, for Gadobenate [29] and Gadoxetate [30], respectively), that, however, is sufficient for generating a plasma relaxivity higher than the ones reported for other first generation GBCAs (Fig. 1B).

An improved albumin-binding Gd-complex is represented by **Gadofosveset** (MS-325) [31], an injectable angiography imaging agent developed in the late nineties by EPIX Medical (formerly Metasyn) and then approved with the name of Vasovist® (Bayer Schering Pharma AG) for use in magnetic resonance angiography in the European Union, Switzerland, Turkey, Australia, and Canada [32]. Later (in 2017) its production was discontinued by the manufacturer due to poor sales. Despite its withdrawal, it remains a reference compound for HSA-binding contrast agents, as its effectiveness (plasma relaxivity measured at 0.5 T and 37 °C, around 40 mM^{-1} s^{-1}) is in the upper range of values ever reported. This value can be accounted for the occurrence of a very strong binding to HSA (K_a = 11 mM^{-1}) [31]. However, all the three agents discussed in this paragraph are derived from the linear Gd-DTPA structure thus endowed with lower kinetic inertness in respect to macrocyclic systems [7].

Derivatives of Gd-DOTA, upon functionalization with benzyloxymethyl [33] or dibenzylamino-methylphosphinate [34] moieties allowed to achieve good binding affinities and relaxivities in the presence of HSA (53.2 and 52 mM^{-1} s^{-1} at 0.47 T and 25 °C for Gd-DOTA $(BOM)_3$ and Gd-DO3A-dibenzylamino, respectively). Analogously Gd-AAZTA, following conjugation with a deoxycholic acid moiety [35] (Gd-AAZTA-MADEC) reached the relaxivity of 38.7 mM^{-1} s^{-1} at 0.47 T and 37 °C.

It should be noted that according to the paramagnetic relaxation theory, the reorientational time of HSA-adducts (approximately 30 ns) predicts much higher relaxivity values (up to ca. 100 mM^{-1} s^{-1}) than those typically observed. Evidence has been gained to show that one reason for the limited relaxation enhancement is often related to a relatively long exchange lifetime (τ_m) of the coordinated water molecule. When rotation slows down upon the formation of a large-sized system, such as an albumin adduct, the exchange rate of the coordinated water molecule may become a limiting factor for the attainment of high relaxivities if it falls outside the optimal range of 10–50 ns at 0.47 T [5]. The clinically approved macrocyclic GBCAs (Gd-DOTA, Gd-HPDO3A, Gd-BT-DO3A) have water exchange dynamics (τ_m in the range 200–300 ns) which becomes sub-optimal when their motion is slowed down upon the formation of protein adducts. The reason for this slow water exchange is that their solution structures adopt mainly a square antiprismatic (SAP) coordination geometry. A second structure is possible for DOTA-like macrocyclic chelates, termed twisted square antiprismatic (TSAP), which, in the above mentioned complexes, is less populated than the first one [36]. It was shown that the water exchange in TSAP isomers is up to 100 times faster than in the SAP isomer [37], thus strategies to design Gd-chelates where the isomers distribution is pushed toward TSAP conformation were intensively pursued [38]. One of these strategies foresees the introduction of bulky substituents on the pendant acetic arms in order to stabilize the preferred TSAP conformation while decreasing the interchange between the two.

Recently, two new α-aryl substituted Gd-DOTA derivatives were reported, in which several key parameters for achieving theoretically high relaxivity were optimized simultaneously [39]. One of these compounds, **Gd-DOTFA**, exhibits preferential TSAP conformation (SAP/TSAP ratio = 1:7), fast water exchange (τ_m = 19 ns), improved electronic relaxation, and moderate binding affinity to serum albumin (K_a = 220 M^{-1}). Theoretical models predict an impressive relaxivity of 110 mM^{-1} s^{-1} (at 0.47 T and 25 °C) when the complex would be fully bound to the protein. However, despite these promising features, the binding affinity to serum albumin appears insufficient to deliver the expected high relaxivity when dissolved in human serum at clinically relevant MRI doses.

Along the same line of reasoning, a lot of efforts has been devoted to the functionalization of Gd-HPDO3A to obtain improved albumin binding Gd-complexes [40–42]. Recently, a new Gd-HPDO3A derivative (**Gd-HIBDO3A-DCA**) [42] was reported where the introduction of an additional methyl group on the hydroxyl arm favored the stabilization of the TSAP structure (SAP/TSAP ratio = 1:8.5 and τ_m = 53 ns) and the presence of a deoxycholic acid residue guaranteed high HSA binding (K_a = 9.1 × 10^4 M^{-1}). Unfortunately, also in this case, the relaxivity measured in human serum (r_1 = 26.8 mM^{-1} s^{-1} at 0.47 T and 25 °C), even if high, is lower than what theoretically expected. The optimized water exchange dynamics, in fact, could not be fully exploited in the formation of the supramolecular adduct with serum albumin due to the occurrence of local flexibility of the protein-bound complex and a slightly increased distance between the gadolinium ion and the water protons ($r_{Gd\text{-}H}$). In fact, it has been shown how the internal rotation of the linker adds flexibility, leading to a shorter effective reorientational correlation time for the Gd-complex compared to the system's global

rotation [43]. Consequently, the increase in molecular size does not result in a proportional reduction of the tumbling motion and, thus, in an effective enhancement of relaxivity [44]. Examples of Gd-complexes with improved relaxivities have been reported, by incorporating linkers that hamper restricted local rotations. A Gd-EGTA (EGTA = ethylene glycol-bis(2-aminoethylether)-N,N,N′,N′-tetraacetic acid) derivative incorporating an aromatic moiety, although with a modest HSA binding affinity (K_a = 8.8 x 10^3 M^{-1}), showed a very high measured relaxivity (80 mM^{-1} s^{-1} at 0.7 T and 25 °C), close to the maximum theoretical one, thanks to the small rotational movements provided by the rigid naphthalene-based binding moiety, as confirmed by molecular docking calculations [45,46].

These findings outline the importance of introducing rigid spacers in the design of GBCAs-binding to proteins.

Other strategies to accelerate water exchange in both linear and macrocyclic Gd^{3+} complexes, rely on the generation of increased steric crowding around the water binding site [47,48] The same approach to enhance water exchange rate was later used to improve the relaxivity of HSA-bound zinc-sensitive agents [49]. As discussed, binding to HSA has typically been achieved by introducing substituents that recognize well-established lipophilic drug-binding sites, known as Sudlow sites I and II, with binding affinities that are also affected by the amount of fatty acids bound to the protein [50]. However, a recently reported approach has explored enhancing relaxation through the set-up of novel noncovalent interactions, such as electrostatic salt bridges and cation−π interactions. This approach leverages the reversible formation of binding motifs with proteins that have abundant positively charged groups exposed on their outer surface.

Cation−π interactions are primarily electrostatic, where a positively charged cation interacts with the negatively charged electron cloud of a π-system. These interactions are notably stronger than typical hydrogen bonds. In this context, a gadolinium-based contrast agent, **Gd-L1**, was synthesized featuring a trisulfonated pyrene derivative of HPTS on its surface [51]. The interaction of this GBCA with proteins presenting many cationic amino groups on their surfaces was then investigated, highlighting this alternative mechanism for generating relaxation enhancement. The presence of a large π-system proved advantageous in facilitating cation-π interactions and forming salt bridges with protonated amino groups on serum proteins (albumin and γ-globulins) as well as extracellular matrix (ECM) proteins like collagen. This resulted in significantly high and concentration-dependent relaxivity, reaching up to 26.5 mM^{-1} s^{-1} at 25 °C and 0.5 T in human serum, and 12.4 mM^{-1} s^{-1} in an ECM-mimicking medium. The efficacy of this contrast agent was further demonstrated *in vivo*, where MRI signal enhancement in the liver, kidneys, and spleen after intravenous administration was up to six times greater than that of the parent compound Gd-HPDO3A, while maintaining an analogous rapid excretion. This increased *in vivo* performance can be attributed to enhanced uptake of Gd-L1 in the extravascular space, where numerous interactions with proteins in the extracellular and extravascular environment may occur. Gd-L1 represents a prototype for a new class of protein binding paramagnetic metal complexes. Such small and hydrophilic agents are capable of establishing weak but abundant interactions with endogenous proteins in both the vascular and ECM environments.

An alternative way to achieve an increase in relaxivity by exploiting the interaction with proteins was proposed some years ago by designing a system in which several units (ca. 10) of **Gd-HPDO3A** are trapped in the inner cavity of **apoferritin** (Fig. 2B) [53]. The objective was to design a system with a large protein surface to facilitate interaction with the paramagnetic complex, impacting a significant number of hydration water molecules and mobile protons. The spherical innner compartment of apoferritin provides enough space to entrap 8–10 contrast agent molecules, while water molecules can freely move in and out of the cavity. As a result, the relaxivity exhibited by each Gd-complex within the apoferritin is remarkably high, reaching approximately 80 mM^{-1} s^{-1} at 0.47 T and 25 °C. This value is nearly 20 times greater than the relaxivity of free Gd-HPDO3A in water and ranks among the highest reported for Gd-complexes containing a single coordinated water molecule.

A further impressive enhancement in relaxivity was recently reported for a gadolinium nanoparticle encapsulated within human H-ferritin nanocage (Gd-HFn) [54]. Gd-HFn, with a mean diameter of approximately 10 nm, were synthesized by loading Gd^{3+} ions into the cavities of HFn nanocages (about 37 Gd ions per nanocage) via diffusion through ion channels, followed by the formation of a Gd nanoparticle (mean diameter ~ 1 nm) within the nucleation site. The claimed relaxivities were as high as r_1 = 549 mM^{-1} s^{-1} per Gd at 1.5 T and r_1 = 428 mM^{-1} s^{-1} per Gd at 3.0 T, surpassing all previously reported values. Although the precise mechanisms underlying this exceptional relaxivity remain unclear, it is likely that the encapsulation of the Gd nanoparticle within the HFn nanocage significantly enhances dipolar interactions between Gd ions and nearby water molecules.

Thanks to the high affinity and specificity of HFn for transferrin receptor 1 (TfR1), which is overexpressed in many tumors and high-risk atherosclerotic plaques, the remarkable MR sensitivity of Gd-HFn enabled the visualization of tumors as small as ~ 2 mm in diameter — approaching the size of the angiogenic switch (1–2 mm) — as well as atherosclerotic plaques, with an administered dose as low as 0.016 mmol Gd/kg. Although the biosafety of this system was evaluated both *in vitro* and *in vivo* through histological analysis of major organs, revealing no pathological abnormalities, further safety studies appear necessary. A 10 % release of Gd^{3+} ions was observed after 60 h of incubation in 10 % mouse serum at 37 °C, an amount that, of course, cannot be considered negligible.

Alternatively to non-covalent interactions, protein-based delivery of paramagnetic probes to achieve high relaxivity can also be accomplished by creating a covalent bond between a suitably modified Gd-complex and reactive sites on proteins [55,56]. An interesting example was reported a few years ago, in which four **Gd-DOTA** derivatives were attached to the tetrameric protein **L-asparaginase II** (ANSII), a biological drug used clinically to treat leukemia (Fig. 2C) [57]. In this way, a relaxivity, at 37 °C and 1 T magnetic field, as large as ca. 35 s^{-1} mM^{-1} was measured.

Another particularly promising approach was pursued by Yang and colleagues, who engineered chimeric proteins incorporating one or more gadolinium-binding sites with high metal selectivity, within a stable and potentially fully functional host protein [52]. This group was very active in the last years and numerous examples of protein-targeted MRI contrast agents (**ProCAs**) have been investigated, where high relaxivity was achieved due to the engineered contributions of a second shell formed by trapped water molecules within the rigid protein environment, a slower rotational correlation time (τ_r = 3–10 ns), and a suitably short water residency time [52]. Particularly interesting systems are those represented by ProCA1 [58], designed by de-novo creating a Gd(III)-binding site on domain 1 of cell adhesion protein (CA1.CD2), and ProCA32s [59], where 2 Gd(III)-binding sites were obtained by reshaping two Ca(II)-binding sites in parvalbumin (Fig. 2D). In ProCA1 (MW ~ 12 kDa), the bound Gd(III) ion exhibits minimal internal tumbling, with a rotational correlation time of approximately 10 ns. The metal ion is coordinated by two inner-sphere water molecules and surrounded by additional second-sphere water molecules. This configuration results in an exceptionally high relaxivity of 117 mM^{-1} s^{-1} at 37 °C and 1.5 T, one of the highest ever reported. However, despite its high relaxivity and strong Gd(III) selectivity over Zn(II), the thermodynamic stability of Gd-ProCA1 required improvement, as its conditional stability constant (log K_{cond}) was only 12.06.

To address this issue, a new system, ProCA32, was developed. In the new design, the coordination spheres of the two Gd(III) ions are nearly fully saturated by oxygen-donor groups from the protein, with a single water molecule in the first coordination shell shared between the two coupled Gd-binding EF-hand sites (0.5 molecules per Gd). While ProCA32 owns a reduced inner-sphere hydration compared to ProCA1, it

features about 10 water molecules hydrogen-bonded to the protein's receptor groups, with an average of 5 molecules per Gd(III). This extensive second-sphere hydration contributes significantly to the relaxivity. As a result, ProCA32 exhibits high relaxivity (30 mM^{-1} s^{-1} at 37 °C and 1.4 T) alongside with exceptional thermodynamic stability (log K_{cond} = 22.5 at pH = 7.2), outperforming both macrocyclic and linear GBCAs, which typically have log K_{cond} values around 17–18. Additionally, ProCA32 demonstrated remarkable selectivity for Gd(III) over Ca(II), Mg(II), and Zn(II), with selectivity values up to 100- to 10^{11}-fold higher than commercial GBCAs. It also exhibits strong kinetic inertness comparable to macrocyclic GBCAs, significantly surpassing that of linear GBCAs. Notably, ProCA32 maintains strong serum stability, remaining intact for over 12 days [52,59].

While Gd-tagged ProCAs seem less suitable for routine contrast-enhanced MRI, they could be highly advantageous for molecular imaging applications. Molecular imaging demands contrast agents with significantly higher relaxivity values than traditional low molecular weight GBCAs, as well as the capacity to target biomarkers specific for a given disease. For providing effective imaging evidence, the contrast between two neighboring areas have to rely on a relaxation rate difference of approximately 0.5 s^{-1}. To cope with this requirement one needs to have, in the region of interest, about 100 μM of contrast agent (CA) with an r_1 of 5 mM^{-1} s^{-1} at 1.5 T. However, the local concentration of Gd(III) required for *in vivo* imaging is generally significantly greater than the natural expression levels of molecular biomarkers. For instance, collagen, a biomarker in tumor microenvironments and liver and lung fibrosis, is generally present at concentrations between 1 and 20 μM. To detect such low biomarker expression levels, a CA must exhibit relaxivity of at least 60 mM^{-1} s^{-1} [60]. To meet this challenge, the ProCA32 platform was engineered with various targeting functionalities designed to bind specific biomarkers such as collagen [61,62], PSMA [63], CXCR4 [60], and HER2 [64]. One notable example is ProCA32.collagen, which selectively targets Collagen I with high affinity (K_d = 1 μM) and specificity over other collagen types(i.e collagens III and IV) [62].

Preclinical studies from the Yang laboratory demonstrated that ProCA32.collagen, with its high relaxivity (30 mM^{-1} s^{-1} at 37 °C and 1.4 T) and a diameter of 2–3 nm, can detect lesions much smaller (100 times) than the detection limits achieved with the current clinical contrast agents. It also shows promise in early-stage detection of liver fibrosis and hepatic cancers, with the ability to visualize lesions as small as 0.2–20 mm in animal models [61]. Furthermore, ProCA32.collagen offers advantages in safety due to its lower dosage requirements, strong resistance to transmetallation, and exceptional metal selectivity for Gd^{3+} over physiological metal ions, making it an excellent candidate for molecular imaging with strong translational potential.

2.1.1.3. – Nanosized Gd-based probes. Another effective strategy to reduce the reorientational mobility of a paramagnetic complex, thereby increasing relaxivity, is to confine the complex within nanosized matrices such as silica or gold nanoparticles, nanostars, nanotubes, self-assembled lipid nanoparticles, or nanogels. As discussed in the previous paragraph, the expected increase in relaxivity can be achieved provided that the exchange dynamics of coordinated water is sufficiently fast.

Although numerous preclinical studies have been conducted to develop and evaluate nanosized Gd-based probes, our focus will be on those that stand out for their exceptional relaxivity enhancement compared to others.

Mesoporous Silica Nanoparticles (MSNs) are among the most promising nanocarriers for various biomedical applications due to their unique structure, which features three distinct domains that can be independently exploited or functionalized, namely the silica framework, the internal pore walls, and the outer surface (Fig. 3A).

This versatility makes MSNs highly adaptable for a wide range of targeted uses [69]. From the relaxometric point of view, it is worth underlining that the position where the Gd-complex is bound, the porosity and the surface chemistry of the mesoporous silica could have a drastic influence on the relaxometric properties of the anchored paramagnetic centers. Higher relaxivity values are indeed achieved i) when the Gd-complex is attached to the external surface of the MSNs (for example, r_1 = 53.6 $mM^{-1}s^{-1}$ at 0.5 T and 37 °C for a Gd-DOTAGA chelate selectively bound to the amino groups on the external surface of MSNs) [65] due to improved water accessibility to the paramagnetic complexes compared to when the probes are confined within the pores; ii) when the pore size increases, allowing better diffusion of water

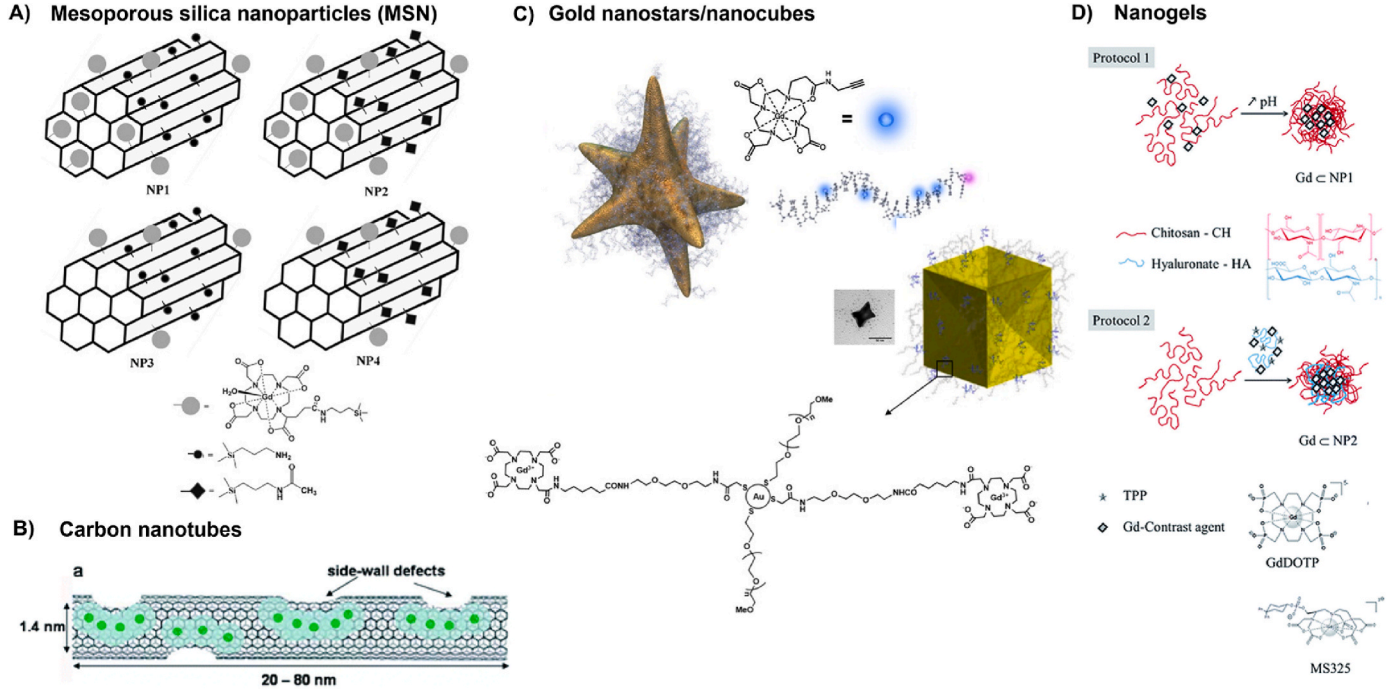

Fig. 3. Examples of slowly tumbling nanosized Gd-based probes. Images reported in A) B) C) and D) were reproduced with permissions from Refs. [65–68], respectively.

molecules through the larger pores [70,71]; iii) when the number of reactive functional groups (such as silanol groups, neutral, or positive species) near the attached paramagnetic chelates is minimized, as seen when the relaxivity of Gd-DOTAGA-containing MSNs rises to 80 $mM^{-1}s^{-1}$ at 0.5 T and 37 °C after unreacted amino groups are converted into neutral acetamide groups [72,73].

A notable example of a paramagnetic amorphous silica MRI probe was created by noncovalently confining Gd-EBPATCN complexes within a nanoporous silica matrix during sol-gel synthesis. When incorporated into 25 nm nanoparticles, these complexes exhibited exceptionally high relaxivity, reaching up to 84 mM^{-1} s^{-1} at 0.82 T and 25 °C. This outstanding relaxometric performance was ascribed to the unique structural and dynamic properties of the nanoparticles [74].

Advances in nanotechnology have devoted significant attention to MRI applications of **carbon-based nanomaterials** [75,76]. Different allotropic forms of carbon can be used to form efficient Gd-based carbon nanomaterials, such as gadonanodiamonds [77,78], gadonanotubes [66,79], gadofullerenes [80,81], or gadographenes [82]. Among the various possibilities, the case of Gd-loaded carbon nanotubes stands out for the impressive relaxivity value which, in turn, has been for long time the highest ever reported for Gd-based systems. Upon the confinement of Gd^{3+} aqua ion clusters within ultra-short single-walled carbon nanotubes (US-tubes, Fig. 3B), linear superparamagnetic molecular magnets were obtained with a per Gd relaxivity value as high as 173 mM^{-1} s^{-1} at 1.5 T and 40 °C [66]. Interestingly, the relaxivity of these gadonanotubes remains unchanged upon increasing the frequency, in contrast to any conventional Gd(III)-based probe. The unprecedentedly high proton relaxivities observed in Gd^{3+}-n@US-tubes have been ascribed to the unique metal-ion environment, where superparamagnetic metal centers interact with a large number of coordinated and exchanging water molecules per Gd^{3+} ion, as well as to an exceptionally high mobility of protons inside the tubes [83]. However, a definitive explanation for both the exceptionally high relaxivity and its unusual dependence on magnetic field strength has yet to be provided.

Interesting investigations on nanoparticle shape effects on proton relaxation were also reported. An example is represented by a nanoconjugate developed by covalently attaching a Gd(III) chelate to thiolated DNA strands, followed by conjugation onto **gold nanostars**, resulting in the DNA-Gd@stars construct (Fig. 3C) [67]. These conjugates demonstrate exceptional r_1, reaching values as high as 98 mM^{-1} s^{-1} at 0.5 T and 25 °C. By analyzing the nuclear magnetic relaxation dispersion (NMRD) data, the researchers credited the outstanding performance of DNA-Gd@stars to a substantially increased contribution from second-sphere relaxivity when compared to spherical contrast agents. Their findings demonstrated that the shape and surface curvature of the nanoparticles influence the arrangement of conjugated DNA strands on the particle surface. This organization plays a crucial role in retaining water molecules near the Gd(III) complexes for up to 10 times longer than typical diffusion would allow, contributing to the enhancement of the observed relaxivity. In a related study, other researchers investigated the relaxometric properties of Gd-loaded concave cube gold nanoparticles (CCGNPs, Fig. 3C) and confirmed that nanoparticles with a negatively curved surface exhibit significantly higher relaxivity (r_1 = 34 mM^{-1} s^{-1}, at 0.61 T and 25 °C) compared to their spherical (convex) counterparts (r_1 = 20.6 mM^{-1} s^{-1}, at 0.47 T and 25 °C) [68]. Analogously to the previous example, the primary factor driving the observed relaxation enhancement is the substantial contribution of second-sphere water molecules interacting with the concave surface of the CCGNPs.

As a further class of nanosized probes, **Nanogels** (NG) containing Gd(III) chelates represent promising hypersensitive MRI probes. In addition to restricting local reorientation due to the encapsulation of the contrast agent, the high water content and increased viscosity within the nanogel matrix contribute to generate good relaxivity enhancements. Most nanogels described in the literature are stabilized by noncovalent interactions, such as ionic bonds, hydrogen bonds, and hydrophobic forces, utilizing biocompatible polymers like chitosan [84] hyaluronic acid [85–87], or polypeptide-based systems [88]. In these systems, ionic or hydrophobic Gd-complexes are employed to promote polymer self-assembly and facilitate the nanogel formation (Fig. 3D). Mixed chitosan-hyaluronate-based nanogels (NGs) containing two different Gd(III) complexes with distinct coordination geometries and hydration states, namely Gd-DOTA (q = 1) and Gd-AAZTA (q = 2), revealed marked relaxivity increases. The relaxivity of NG/Gd(DOTA) was 28.6 mM^{-1} s^{-1} at 0.47 T and 25 °C, while NG/Gd(AAZTA exhibited a relaxivity of 62.4 mM^{-1} s^{-1} at the same experimental conditions [86]. This doubling in relaxivity is consistent with the presence of two coordinated water molecules in Gd-AAZTA compared to just one occurring in Gd-DOTA. Quite surprisingly, instead, is the relaxation efficiency shown by chitosan-hyaluronate nanogels containing Gd(DOTP), a complex lacking any metal-bound water molecules (q = 0). Two studies were reported where very similar Gd(DOTP) containing nanogels were characterized, and the relaxivity were determined to be 98 mM^{-1} s^{-1} (0.47 T, 37 °C) [85] and 78 mM^{-1} s^{-1} (0.47 T, 25 °C) [87]. Although the relaxivity values of the two systems differ, both are substantially higher than those measured for mono- or bis-hydrated complexes within the same nanogel. Tentatively, the observed high relaxivity was accounted in terms of the large number of water molecules present in the bulk phase of the nanogel, which engage in strong and long-lived hydrogen bonding interactions within the second coordination sphere of the complex.

2.1.2. How far have we advanced in optimizing hydration (inner and second sphere)?

As shown above, much work devoted to the search of high relaxivities has been done by increasing water exchange rate and reducing molecular tumbling rate, but the hydration state (number and position of the water molecules in the inner coordination sphere) can affect as well the maximum achievable relaxivity [89]. Using hepta- or hexa-dentate ligands, instead of the traditional octa-dentate ones, enables the synthesis of Gd(III) complexes with 2 or 3 coordinated water molecules, respectively, providing a clear advantage in terms of relaxation enhancement as relaxivity scales up with the number of coordinated water molecules (see Equation (2)). However, reducing the ligand denticity often compromises the thermodynamic stability of the resulting metal complexes, potentially increasing their toxicity. Moreover, systems with q = 2 may experience a 'quenching' effect on relaxivity when interacting with endogenous anions (carbonate, phosphate, lactate …) [90,91] or donor atoms from Asp or Glu on proteins [92], as these groups can displace the coordinated water molecules from the metal inner coordination sphere. However, several stable and inert Gd(III) chelates with two inner-sphere water molecules, such as Gd-PCTA [93], Gd-HOPO [94], Gd-AAZTA [95], Gd-Py (Py = 2,6-pyridine-diylbis(methylene nitrilo)] tetraacetate) [96], and their numerous derivatives, have been identified (see Fig. 4) and are being closely studied [97–99]. Notably, a derivative of Gd-PCTA, **Gadopiclenol**, has recently been introduced into clinical practice. It provides relaxivity values of 12.5 mM^{-1} s^{-1} in water and 13.2 mM^{-1} s^{-1} in human serum at 0.47 T and 37 °C. These values are 2–4 times higher than those of "first-generation" GBCAs, the increase being largely ascribed to its doubled inner-sphere hydration. These findings prompted the study of pyclen-based complexes, particularly aiming to understand and optimize the thermodynamic stability and kinetic inertness of the resulting Gd complexes. Recently, it was discovered that adding two ethyl groups to the ethylene moiety of the pyclen backbone, creating a chiral ligand known as **X-PCTA-2**, significantly enhances both relaxivity (6.5 vs. 5.1 mM^{-1} s^{-1} at 1.41 T and 37 °C) and thermodynamic stability (log K_{Gd-L} = 21.3 vs. 20.4) of the resulting Gd complex compared to the parent Gd-PCTA [100].

Interesting (and surprising) observations were reported in a study where it was found that reducing the denticity of the ligand leads to a significant enhancement in kinetic inertness. In an attempt to explore

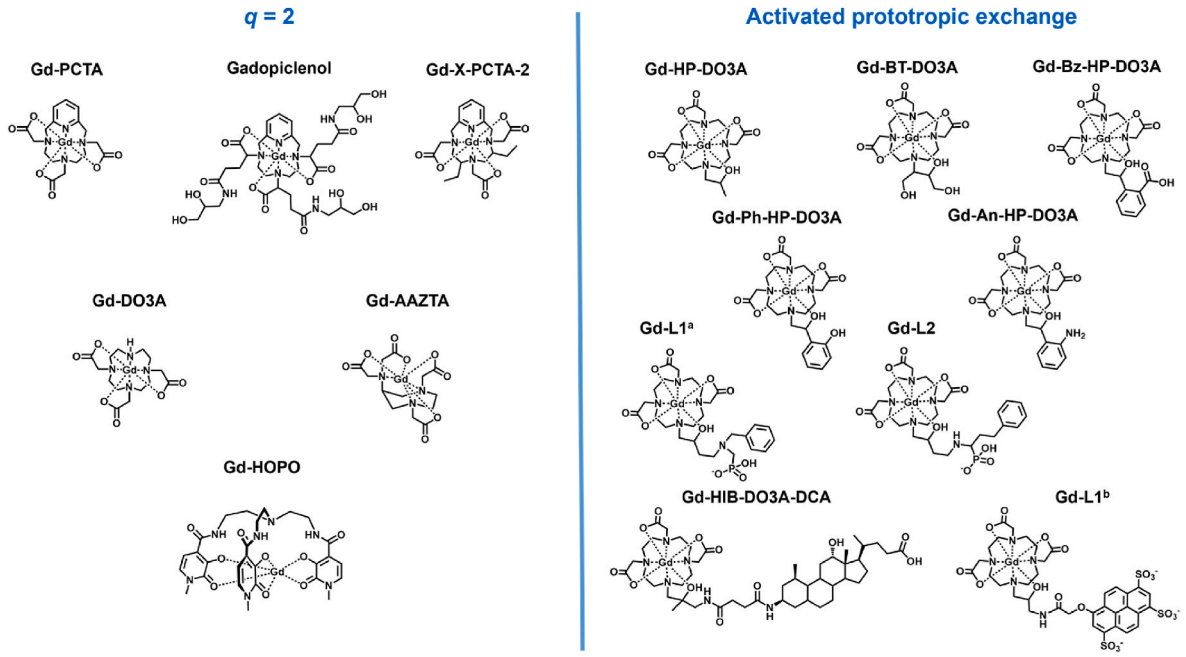

Fig. 4. Structures of representative Gd-complexes with two inner sphere water molecules (left) or with activated prototropic exchange (right). Gd-L1[a] and Gd-L2 from Ref. [109], Gd-HIBDO3A-DCA from Ref. [42], and Gd-L1[b] from Ref. [51].

new ligand frameworks for obtaining stable and inert bis-hydrated Gd-complexes, three chiral ligands featuring a highly rigid (1S,2S)-1,2-cyclobutanediamine spacer, along with varying numbers of acetate and picolinate groups, were synthesized [101]. Potentiometric studies revealed similar thermodynamic stability for the Gd^{3+} complexes formed with either the octadentate $(L3)^{4-}$ or the heptadentate $(L2)^{4-}$ analogues (log KGdL = 17.41 for Gd(L2) and 18.00 for Gd(L3)). Furthermore, the monohydrated Gd(L3) complex was found to be much more labile than the bishydrated Gd(L2). Although the inertness of Gd(L2) is not sufficient for practical *in vivo* MRI contrast agent applications, this complex represents an unusual case where a decrease in ligand denticity leads to a significant increase in kinetic inertness.

Some attempts have been made to increase the hydration number to $q = 3$ in Gd complexes, consistently leading to higher relaxivity [102,103]. However, these Gd complexes have invariably lacked sufficient thermodynamic stability and kinetic inertness, rendering them unsuitable for use as effective contrast agents *in vivo*.

An alternative approach to enhance relaxivity by increasing hydration, while preserving the high denticity of the ligand and ensuring stability, has been extensively explored by optimizing second-sphere hydration [13]. The second-sphere contribution to relaxivity occurs only when the residence lifetime of structured water in the second coordination shell is longer than the diffusion correlation time. This is made possible by hydrogen bonding interactions with polar groups on the outer surface of the ligand. Extensive research has explored various hydrogen-bond-acceptor groups to optimize this effect, including phosphinate [104], phosphonate [105,106], carboxylate [107], diols and hydroxyl pendant arms [108]. These modifications have consistently led to enhanced relaxivity beyond what is expected from inner- and outer-sphere contributions alone. For instance, Gadopiclenol not only benefits from increased molecular weight and inner-sphere hydration, but its relaxivity receives also a significant contribution from the second-sphere water molecules. This is due to the presence of three isoserinol arms on the ligand, which effectively capture hydrogen-bonded water molecules. The increased rotational correlation time further amplifies the second-sphere relaxivity effect, as demonstrated by the examples discussed in paragraph 1.1. In these cases, the formation of supramolecular nanosized systems results in exceptionally high relaxivity, which can be attributed entirely [59,85,87] or largely [66–68] to the presence of second-sphere water molecules.

2.1.3. *Increased relaxivity by catalysis of the prototropic exchange*

In principle, the exchange of mobile protons from the ligand of a Gd(III) complex with the bulk water is an additional process to enhance the nuclear relaxation rate of solvent water protons. Among clinically approved GBCAs, Gd-HPDO3A and Gd-BT-DO3A are neutral complexes, where the Gd(III) coordination sphere consists of four nitrogens from the macrocyclic ring, three oxygens from the acetic arms, a hydroxyl group, and a water molecule. Although there has been limited research on exploiting this contribution in Gd-BT-DO3A and its derivatives, significant work has been carried out on Gd-HPDO3A and its related compounds (Fig. 4).

Typically, the hydroxyl proton of Gd-HPDO3A is involved in a slow exchange with the bulk water at physiological pH (too slow to affect the relaxivity) while the exchange is catalyzed at basic pH conditions (at pH $\sim$ 10, the proton exchange contribution leads to a $\Delta r_1 = +1.2\ mM^{-1}\ s^{-1}$, at 0.47 T and 25 °C) [110]. However, studies have demonstrated that the proton exchange of the hydroxyl group can be accelerated also at neutral pH by basic components in buffers such as phosphate, carbonate, and HEPES [110,111]. Additionally, introducing appropriate functional groups (e.g., phenol, carboxylate, amine, amide) near the coordinating hydroxyl moiety can facilitate the formation of intramolecular hydrogen bonds with the hydroxyl moiety, further influencing the proton exchange rate, thus enhancing the observed relaxivity (Table 1) [109,112,113]. The beneficial contribution to relaxivity afforded by accelerated prototropic exchange is even more evident when the relaxivity is measured in human plasma. In fact, evidence has been gained to show that an improved relaxivity is obtained in biological fluids due to both slowing down the rotational dynamics and an activated contribution from exchangeable protons [42,51,109].

2.2. *Optimized relaxivity at high magnetic fields*

Magnetic resonance scanner technology has advanced significantly, with field strengths rising from 0.1 T in the 1980s to modern clinical MRI systems operating at 1.5–3 T and with 7 T scanners recently approved

Table 1
List of GBCAs discussed in this review and their principal relaxometric parameters and characteristics.

	GBCA	r_1 Relaxivity ($mM^{-1}s^{-1}$)	q	τ_R	τ_M	2nd sph	Features	Ref
First generation GBCAs	**Gadopentetate**	3.4 (water, 0.47 T, 37 °C) 3.1 (water, 3 T, 37 °C) 3.8 (plasma, 0.47 T, 37 °C) 3.7 (plasma, 3 T, 37 °C)	1	58 ps (25 °C)	130 ns (37 °C)	no	General purpose	[17, 23]
	Gadodiamide	3.5 (water, 0.47 T, 37 °C) 3.2 (water, 3 T, 37 °C) 4.4 (plasma, 0.47 T, 37 °C) 4.0 (plasma, 3 T, 37 °C)	1	66 ps (25 °C)	1 μs (37 °C)	no	General purpose	[17, 23]
	Gadobenate	4.2 (water, 0.47 T, 37 °C) 4.0 (water, 3 T, 37 °C) 9.2 (plasma, 0.47 T, 37 °C) 5.5 (plasma, 3 T, 37 °C)	1	88 ps (25 °C)		no	Hepatospecific, weak HSA binding	[17, 23]
	Gadoxetate	5.3 (water, 0.47 T, 37 °C) 4.3 (water, 3 T, 37 °C) 8.7 (plasma, 0.47 T, 37 °C) 6.2 (plasma, 3 T, 37 °C)	1	178 ps (25 °C)	124 ns (37 °C)	no	Hepatospecific, weak HSA binding	[17, 23]
	Gadoterate	3.4 (water, 0.47 T, 37 °C) 2.8 (water, 3 T, 37 °C) 4.3 (plasma, 0.47 T, 37 °C) 3.5 (plasma, 3 T, 37 °C)	1	77 ps (25 °C)	108 ns (37 °C)	no	General purpose	[17, 23]
	Gadoteridol	3.1 (water, 0.47 T, 37 °C) 2.8 (water, 3 T, 37 °C) 4.8 (plasma, 0.47 T, 37 °C) 3.7 (plasma, 3 T, 37 °C)	1			no	General purpose	[17, 23]
	Gadobutrol	3.7 (water, 0.47 T, 37 °C) 3.2 (water, 3 T, 37 °C) 6.1 (plasma, 0.47 T, 37 °C) 5.0 (plasma, 3 T, 37 °C)	1			no	General purpose	[17, 23]
Prototropic exchange	**Gd-BzHPDO3A**	4.3 (water, 0.47 T, 37 °C) 6.5 (plasma, 0.47 T, 37 °C)	1			no	Low MW, activated prototropic exchange	[112]
	Gd-PhHPDO3A	4.9 (water, 0.47 T, 37 °C) 9.1 (plasma, 0.47 T, 37 °C)	1			no	Low MW, activated prototropic exchange	[112]
	Gd-BzHPDO3A	4.7 (water, 0.47 T, 37 °C) 7.3 (plasma, 0.47 T, 37 °C)	1			no	Low MW, activated prototropic exchange	[112]
	GdL1[a]	7.1 (water, 0.47 T, 37 °C) 10.9 (plasma, 0.47 T, 37 °C)	1			no	Low MW, activated prototropic exchange	[112]

(*continued on next page*)

Table 1 (*continued*)

		GBCA	r_1 Relaxivity ($mM^{-1}s^{-1}$)	q	τ_R	τ_M	2nd sph	Features	Ref
		GdL2	8.3 (water, 0.47 T, 37 °C) 12.5 (plasma, 0.47 T, 37 °C)	1			no	Low MW, activated prototropic exchange	[112]
Larger MW		**Gadopiclenol**	12.5 (water, 0.47 T, 37 °C) 11.3 (water, 3 T, 37 °C) 13.2 (plasma, 0.47 T, 37 °C) 11.6 (plasma, 3 T, 37 °C)	2	139 ps (37 °C)	85.8 ns (37 °C)	yes	General purpose, bishydrated, 2nd sphere, intermediate/low MW	[21, 24]
		Gadoquatrane	10.6 (water, 0.47 T, 37 °C) 9.9 (water, 3 T, 37 °C) 12.5 (plasma, 0.47 T, 37 °C) 10.5 (plasma, 3 T, 37 °C)	1			no	General purpose, tetrameric structure, interm. MW	[22]
		P846	24.0 (water, 3 T, 37 °C)	2			no	Bishydrated, interm./high MW	[25]
		P792	39.0 (water, 0.47 T, 37 °C) 12.0 (water, 3 T, 37 °C)	1	1.7 ns (37 °C)	96 ns (37 °C)	yes	2nd sphere, High MW	[26]
		EP2104R	11.1 (water, 0.47 T, 37 °C)	1			no	interm./high MW, fibrin targeting	[28]
Adducts with proteins	**Non covalent adducts**	**Gadofosveset (MS325)**	6.84 (water, 0.47 T, 37 °C) 5.47 (water, 1.4 T, 37 °C) 50.1 (HSA, 0.47 T, 37 °C)	1	115 ps (free, 37 °C) 10.1 ns (bound, 37 °C)	69 ns (free, 37 °C) 170 ns (bound, 37 °C)	no	Strong HSA binding, angiography	[31]
		Gd-DOTA(BOM)$_3$	53.2 (HSA, 0.47 T, 25 °C)	1			no	Strong HSA binding	[33]
		Gd-DO3A-dibenzylamino	5.5 (water, 0.47 T, 25 °C) 52 (HSA, 0.47 T, 25 °C)	1	92 ps (free, 37 °C)	5 ns (free, 37 °C)	yes	Intermediate HSA binding, fast water exchange, 2nd sphere	[34]
		Gd-AAZTAMadec	13.9 (water, 0.47 T, 25 °C) 38.7 (HSA, 0.47 T, 37 °C)	2	200 ps (free, 25 °C) τ_R^L = 460 ps (25 °C) τ_R^G = 6 ns (25 °C)	100 ns (free, 25 °C)	no	Strong HSA binding, bishydrated	[35]
		Gd-DOFTA	8.1 (water, 0.47 T, 25 °C) 110 (HSA, 0.47 T, 25 °C)	1	161 ps (free, 25 °C)	19 ns (free, 25 °C)	no	Weak HSA binding, fast water exchange	[39]
		Gd-HIBDO3A-DCA	8.1 (water, 0.47 T, 25 °C) 26.8 (HSA, 0.47 T, 25 °C)	1	170 ps (free, 25 °C) τ_R^L = 527 ps (25 °C) τ_R^G = 30 ns (25 °C)	53 ns (water, 25 °C) 18 ns (serum, 25 °C)	no	Strong HSA binding, fast water exchange, prototropic exchange	[42]
		Gd-EGTA-naftalene	5.7 (water, 0.47 T, 25 °C) 68 (HSA, 0.47 T, 25 °C)	1	58 ps (free, 25 °C) τ_R^L = 6 ns (25 °C) τ_R^G = 41 ns (25 °C)	18 ns (25 °C)	no	Intermediate HSA binding, solidal tumbling with HSA	[45, 46]
		Gd-L1	7.1 (water, 0.47 T, 25 °C) 26.5 (serum, 0.47 T, 25 °C)	1	115 ns (25 °C)	189 ns (25 °C)	yes	Weak HAS binding, 2nd sphere, prototropic exchange	[51]
	Inclusion/ covalent binding	**Gd-HPDO3A/ Apoferritin**	80 (0.47 T, 25 °C)	1			no	High MW, compartimentalized	[53]
		Gd-HFn	549 (1.5 T, 25 °C)				no	High MW, compartimentalized	[54]
		Gd-DOTA-ANSII	35 (1 T, 37 °C)	1	3.4 ns (37 °C)	230 ns (37 °C)	no	Covalently bound to the protein	[57]

(*continued on next page*)

Table 1 (*continued*)

	GBCA	r_1 Relaxivity ($mM^{-1}s^{-1}$)	q	τ_R	τ_M	2nd sph	Features	Ref
	ProCA1	117 (1.5 T, 37 °C)	2			yes	High MW, 2nd sphere, used for targeted molecular imaging	[58]
	ProCA32s	30 (1.4 T, 37 °C)	0			yes	High MW, 2nd sphere, used for targeted molecular imaging	[59]
Nanosized systems	**Gd-DOTAGA-NP3**	53.6 (0.5 T, 37 °C)	1	τ_R^L = 3.7 ns (37 °C) τ_R^G = 0.1 ms (37 °C)	160 ns (37 °C)	no	High MW, Bound to MSN	[65]
	Gd-DOTAGA-NP4	80.0 (0.5 T, 37 °C)	1	τ_R^L = 3.0 ns (37 °C) τ_R^G = 0.1 ms (37 °C)	36 ns (37 °C)	no	High MW, Bound to MSN, fast water exchange	[65]
	Gd-EBPATCN-MSN	84.0 (0.82 T, 25 °C)	1			no	High MW, bound to MSN	[74]
	Gd-n@US-tubes	173 (1.5 T, 40 °C)				yes	High MW, compartimentalized, 2nd sphere, prototropic exchange	[66]
	DNA-Gd@stars	98 (0.75 T, 25 °C)	1	>1000 ns (37 °C)	22 ns (37 °C)	yes	High MW, fast water exchange, negative surface curvature facilitate 2nd sphere	[67]
	NG/Gd-DOTA	28.6 (0.47 T, 25 °C)	1	120 ns (37 °C)	6 ns (37 °C)	no	High MW, fast water exchange	[86]
	NG/Gd-AAZTA	62.4 (0.47 T, 25 °C)	2	190 ns (37 °C)	4.4 ns (37 °C)	no	High MW, fast water exchange, bis-hydrated	[86]
	NG/Gd-DOTP	98 (0.47 T, 25 °C)	0			yes	High MW, 2nd sphere	[85]

for clinical applications [114]. Experimental scanners for both animal and human studies now reach field strengths as high as 9.4 T [115,116] and 11.7 T [117]. At higher fields a greater signal-to-noise ratio (SNR), higher spatial resolution and reduced acquisition times can be achieved. Consequently, the development of contrast agents optimized for higher magnetic fields has become a crucial task in designing next-generation, highly efficient MRI probes.

The theory on the interactions between a paramagnetic center and the water protons relies on the Solomon-Bloembergen-Morgan equations (paragraph 1.1) containing field/frequency-dependent contributions from dipolar and scalar interactions. As a consequence, the relaxivity of a given GBCA results to be field-strength dependent, with reduction up to ca. 50 % between 0.47 and 7 T for commercial GBCAs (Fig. 5) [23,118,119].

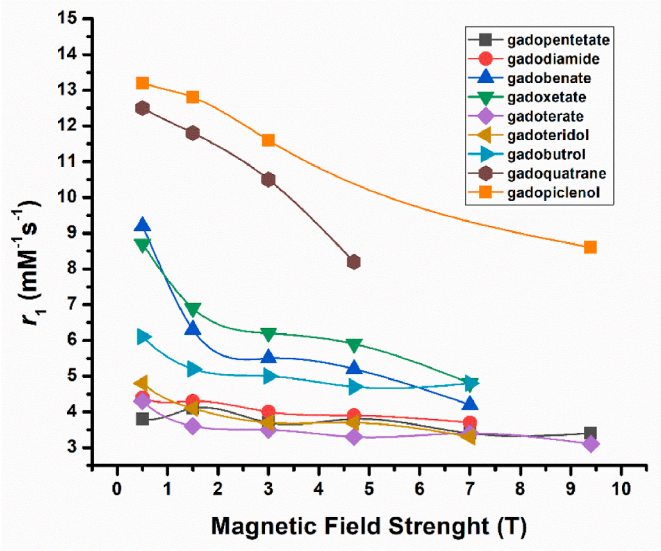

Fig. 5. Longitudinal proton relaxivities (mM^{-1} s^{-1}) of commercial GBCAs measured in plasma at 37 °C as a function of increasing magnetic field strength. Relaxivity values up to 4.7 T are from Refs. [22,23], at 7 T from Ref. [118], and at 9.4 T from Ref. [119].

As a consequence, the optimal correlation times for maximizing relaxivity at 0.5 T differ from those that yield the highest relaxivity at 3–7 T.

While for small, fast tumbling molecules the decrease in r_1 with field is modest, for slowly tumbling molecules (τ_r = 10–30 ns), like GBCAs bound to serum albumin, the high relaxivities that peak between 0.5 and 1 T sharply drop with increasing field. As nicely illustrated in a review by Caravan et al., [31] the strategy of markedly slowing rotational motion results in large gains in r_1 at 0.5–1.5 T, but at high fields is much less effective.

To obtain good relaxivity over the 1.5–7 T range, intermediate rotational correlation times in the range 0.5–1.5 ns are most effective while the water exchange rate is not as critical as at lower fields. Moreover, as the inner- and second-sphere contributions to relaxivity scale linearly with the number of water molecules and are field independent, a higher hydration number would be beneficial at any field strength. Moreover, although very high relaxivity is theoretically possible at low fields, it requires a narrow range of correlation times (τ_R and τ_M), making it difficult to achieve, whereas higher fields allow good relaxivity across a broader range of exchange rates and dynamics [31].

Intermediate rotational correlation times are usually associated to rigid, medium sized (MW = 2–6 kDa) poly-nuclear Gd-complexes. Several examples are available, either based on self-assembly or on covalent conjugation of Gd-chelates to a rigid core, for which increased high-field relaxivity has been reported [120,121]. It has been shown in high field MR imaging that the enhanced relaxation efficiency is retained *in vivo* [122]. In a study by Tei et al., [123] the relationship between relaxivity at high magnetic fields and rotational dynamics was explored using a homogeneous series of multimeric structures with molecular weights ranging from approximately 600 to 6000 Da. These structures consist of one to eight bis-hydrated Gd(AAZTA) complexes, linked via a central scaffold with a spacer designed to minimize internal rotation. The researchers found that relaxivity per Gd ion increased significantly, at 1.5 T and 298 K, from the monomer to the hexanuclear complex, with a remarkable 370 % enhancement. However, at 3 T, a linear increase in relaxivity was observed only up to the tetrameric structure, and at fields approaching or exceeding 7 T, no significant difference in relaxivity was noted between the trimer, tetramer, and hexamer. The authors concluded that the Gd_3L3 complex (MW ~ 2 kDa) offered an excellent balance, displaying high relaxivity that remained

largely unaffected by increasing magnetic field strength (r_1 per Gd ~ 15 mM^{-1} s^{-1}, in the field range 0.5–7 T).

Another noteworthy example of sustained high relaxivity at elevated magnetic fields is the ProCA1 Gd-coordinating protein, discussed in paragraph 1.1.2 [58]. In ProCA1 (MW ~ 12 kDa), the bound Gd(III) ion experiences minimal internal tumbling, with a rotational correlation time around 10 ns. Although this value lies outside the optimal range for maximizing relaxivity at high fields (typically 0.5–1.5 ns), the r_1 values measured at 3 T and 9.4 T–48 mM^{-1} s^{-1} and 6 mM^{-1} s^{-1}, respectively — are still considered impressive and demonstrate strong performance under these conditions.

The search for intermediate-sized Gd-based probes can also be extended to small nanoparticles, just a few nanometers in size. A notable example is AGuIX®, an ultra-small nanoparticle with a polysiloxane core surrounded by 10 Gd-DOTA complexes on its periphery [124]. With a hydrodynamic diameter of about 3 nm and a molecular mass of 8.5 kDa, AGuIX is small enough for rapid renal excretion, avoiding accumulation in RES macrophages. AGuIX demonstrates a two-fold increase in r_1 relaxivity (6.0 mM^{-1} s^{-1}) at 7 T per Gd(III) ion compared to Gd-DOTA (3.0 mM^{-1} s^{-1}). Additionally, its superior contrast enhancement properties were confirmed at 9.4 T, where it more effectively distinguished hepatic tumors from normal tissue compared to Gd-DOTA [125].

In another approach, high-field relaxivity was optimized by the self-assembly of two macrocyclic Gd(III) complexes, resulting in a small-sized dimeric system. Specifically, dimeric Gd(III) compounds were formed by using two pendant phosphate groups on a monoamide derivative of Gd-DOTA, which bind to the inner coordination sphere of a monomeric Gd-DO3A-type diaqua complex [126]. This assembly led to significantly enhanced relaxivities over a wide range of magnetic fields, due to improved inner- and second-sphere contributions. At clinically relevant magnetic fields (0.5–3 T), the relaxivity of the dimer reaches approximately 18 mM^{-1} s^{-1} (at 25 °C), which is substantially higher than the sum of the individual relaxivities of the two Gd complexes (6.2 mM^{-1} s^{-1} for the Gd-DOTA derivative and 7 mM^{-1} s^{-1} for the Gd-DO3A derivative). This increase is attributed to the formation of a compact, rigid structure with an optimized rotational correlation time (~0.2 ns) and an additional contribution (about 30–40 %) from water molecules in the second coordination sphere. The face-to-face dimer conformation facilitates the formation of a hydrogen-bonded network of water molecules around the hydrophilic components of the two chelating units, further enhancing the relaxivity.

2.3. *Pharmacokinetic considerations: low-molecular-weight vs. nanosized GBCAs*

While substantial efforts have been made to optimize the relaxivity of GBCAs through molecular and supramolecular strategies, pharmacokinetics remains a critical parameter influencing both clinical utility and safety. The pharmacokinetic profile determines biodistribution, circulation time, excretion pathways, and ultimately, imaging efficacy and toxicity.

Low-Molecular-Weight GBCAs, such as gadopentetate and gadoteridol, are rapidly excreted via the kidneys and have short plasma half-lives (typically ~1.5 h in individuals with normal renal function) due to their small size (<1 kDa) and high hydrophilicity [127]. This fast clearance makes them ideal for dynamic and routine imaging but limits their capacity for blood pool imaging or targeted molecular applications, where longer systemic retention is desirable.

In contrast, nanosized Gd-based systems, including nanoparticles, protein-based constructs (e.g., ProCA32, HFn), and dendrimers, have significantly larger hydrodynamic diameters (>3 nm), leading to prolonged circulation times and enhanced passive or active accumulation at target sites [128]. Their slower clearance often involves hepatic or reticuloendothelial system (RES) pathways, rather than renal excretion, which raises concerns over prolonged tissue retention and potential toxicity [129].

An important advantage of nanosized systems is their ability to exploit the enhanced permeability and retention (EPR) effect, which facilitates accumulation in tumors or inflamed tissues due to abnormal vasculature and poor lymphatic drainage [130].

Finally, surface modifications, including PEGylation [131] or zwitterionic coatings [132], are crucial in minimizing non-specific uptake by the RES and prolonging blood circulation. Surface charge and hydrophilicity also impact opsonization and immune recognition, affecting the pharmacokinetic profile and biodistribution of nanosized agents [133].

In conclusion, while nanosized agents offer superior relaxivity and targeting capabilities, their more complex pharmacokinetics demand careful design to ensure both efficacy and safety in clinical applications.

3. Conclusions

The huge work done over the last four decades has shown that optimized relaxivities can be obtained by proper control of the various determinants. In the case of macrocyclic GBCAs based on the DOTA-like architecture, a crucial step to attain optimally short exchange lifetimes for the coordinated water deals with the control of the TSAP/SAP geometry. Basically, it has been found that a preferential TSAP conformation can be achieved by substituting protons on the α-carbon of the coordinating arms. The task of slowing down the molecular reorientational motion can be tackled either by increasing the size of the GBCA or by introducing suitable substituents on the ligand surface able to promote the formation of supramolecular adducts with endogenous or exogenous macromolecular substrates. Actually, the two newly introduced second generation GBCAs, Gadopiclenol and Gadoquatrane, display a relaxivity that is 2–3 times the one of the first generation GBCAs and some of the herein reviewed systems investigated at the preclinical level have relaxivities very close to the maximum theoretical values (Fig. 6). Thus, it is evident that much room is still available, in principle, to go for new structures with optimized relaxivity.

Moreover, it is noteworthy to recall that relaxivity is dependent on the magnetic field strength at which it is measured, with the optimal correlation times for maximizing it at 0.5 T differing from those that yield the highest relaxivity at 1.5–3 T. On the other hand, although very high relaxivity is theoretically possible at low fields, it requires a narrow range of correlation times (τ_R and τ_M), making it difficult to achieve, whereas higher fields allow still good relaxivity across a broader range of exchange rates and dynamics [27].

From a pharmacokinetic standpoint, a critical distinction must be made between Low-Molecular-Weight (LMW) GBCAs and emerging nanosized systems. While LMW agents are rapidly cleared by the kidneys and exhibit short circulation times, features that make them well-suited for routine diagnostic imaging, their limited blood residence time can reduce effectiveness in molecular targeting applications. In contrast, nanosized contrast agents, including protein-based platforms and nanoparticles, benefit from prolonged circulation and enhanced tissue accumulation, particularly via the enhanced permeability and retention (EPR) effect. However, these systems often rely on hepatic or RES clearance pathways and may pose greater challenges in terms of long-term safety and gadolinium retention. Therefore, alongside relaxivity optimization, careful consideration of pharmacokinetic behavior, coordination chemistry, stability, biodistribution, and excretion profiles is essential when designing next-generation contrast agents to ensure both imaging efficacy and clinical safety.

In principle, despite the absence of clinically relevant consequences of the tiny amounts of GBCAs retained in the body, it appears reasonable to reduce the administered dose with the newly developed GBCAs, and it is thus a significant step ahead in the context of clinical settings. Of course, one of the main obstacles to the entrance of new efficient GBCAs in the clinical practice is represented by the huge costs any new agent has to tackle for its industrial/clinical translation.

However, it is important that basic research continues to identify

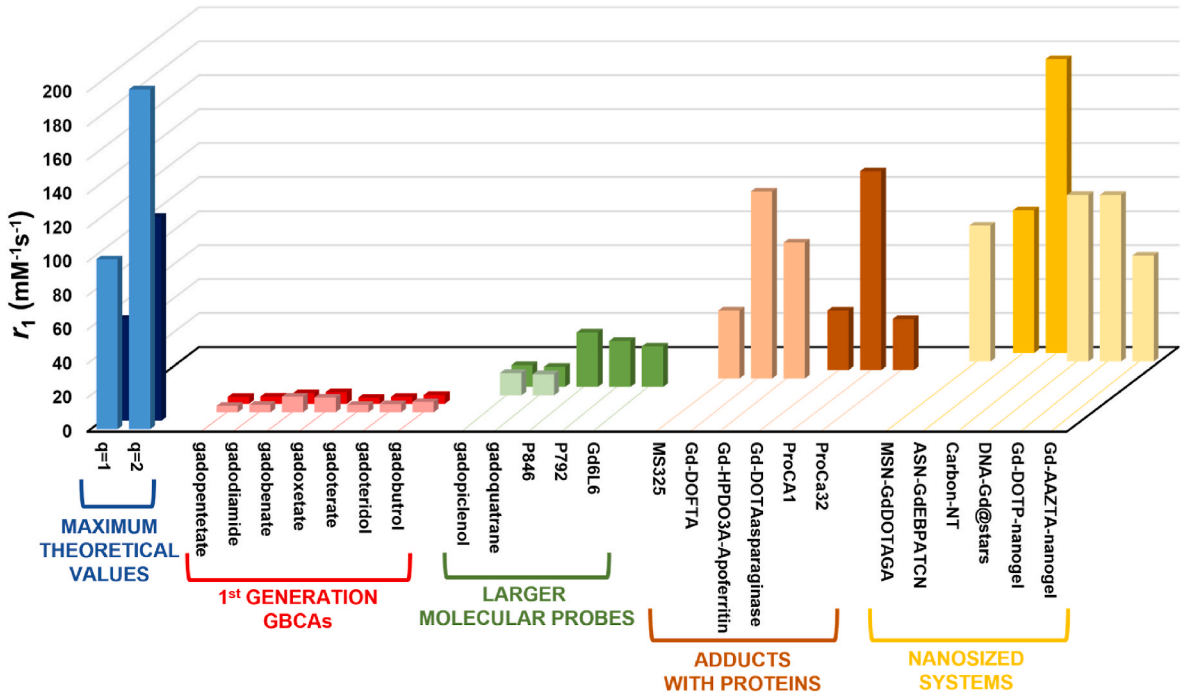

Fig. 6. Longitudinal proton relaxivities (mM^{-1} s^{-1}) of various Gd-based probes discussed in this review at 0.5 T (light colors) and 1.5 T (dark colors), categorized by the strategies used to slow down rotational motion. (For interpretation of the references to color in this figure legend, the reader is referred to the Web version of this article.)

new routes to further improve the relaxivity for GBCAs, as well as for Fe (III) and Mn(II) systems which are currently under scrutiny. The examples provided by compartmentalized systems suggest that much higher relaxivities could be attained. The in-depth understanding of the structural and dynamic determinants of the outstanding relaxation enhancement reported for these systems will be crucial for the rational design of next generation of MRI CAs. The domain of Molecular Imaging will also largely benefit from these efforts.

CRediT authorship contribution statement

Lorenzo Palagi: Writing – review & editing, Formal analysis, Data curation. **Dario Livio Longo:** Writing – review & editing, Formal analysis, Data curation. **Éva Tóth:** Writing – review & editing, Formal analysis, Data curation. **Carlo C. Quattrocchi:** Writing – review & editing, Data curation, Conceptualization. **Aart J. van der Molen:** Writing – review & editing, Data curation, Conceptualization. **Silvio Aime:** Writing – review & editing, Data curation, Conceptualization. **Eliana Gianolio:** Writing – review & editing, Writing – original draft, Validation, Supervision, Data curation, Conceptualization.

Declaration of generative AI and AI-assisted technologies in the writing process

During the preparation of this work the author(s) used ChatGPT in the writing process to improve the readability and language of the manuscript. After using this tool, the author(s) reviewed and edited the content as needed and take(s) full responsibility for the content of the published article.

Funding

This research did not receive any specific grant from funding agencies in the public, commercial, or not-for-profit sectors.

Declaration of competing interest

The authors declare that they have no known competing financial interests or personal relationships that could have appeared to influence the work reported in this paper.

Acknowledgements

The ESMRMB-GREC (Gadolinium Research&Education Committee) is a multidisciplinary group of ESMRMB members, including clinicians, scientists, chemists, physicists, pathologists, and clinical epidemiologists who all share a common interest in the study of GBCAs in a wide variety of clinical and preclinical conditions. The authors thank all the members for their insights based on their specific competence and experience. The list of authors includes the members who developed the project and those experts who have revised and approved the final version of the manuscript.

Data availability

No data was used for the research described in the article.

References

[1] P.A. Rinck, Magnetic Resonance in Medicine, ABW-Wiss.-Verlag, 2003.
[2] J.-C.G. Bünzli, G.R. Choppin, Lanthanide Probes in Life, Chemical, and Earth Sciences: Theory and Practice, Elsevier, 1989.
[3] A.S. Merbach, L. Helm, É. Tóth, The Chemistry of Contrast Agents in Medical Magnetic Resonance Imaging, John Wiley & Sons, 2013.
[4] S. Aime, M. Botta, M. Fasano, E. Terreno, Lanthanide(III) chelates for NMR biomedical applications, Chem. Soc. Rev. 27 (1998) 19–29, https://doi.org/10.1039/A827019Z.
[5] J. Wahsner, E.M. Gale, A. Rodríguez-Rodríguez, P. Caravan, Chemistry of MRI contrast agents: current challenges and new frontiers, Chem. Rev. 119 (2019) 957–1057, https://doi.org/10.1021/acs.chemrev.8b00363.
[6] J. Endrikat, S. Dohanish, N. Schleyer, S. Schwenke, S. Agarwal, T. Balzer, 10 years of nephrogenic systemic fibrosis: a comprehensive analysis of nephrogenic systemic fibrosis reports received by a pharmaceutical Company from 2006 to 2016, Investig. Radiol. 53 (2018) 541, https://doi.org/10.1097/RLI.0000000000000462.

[7] T. Frenzel, P. Lengsfeld, H. Schirmer, J. Hütter, H.-J. Weinmann, Stability of gadolinium-based magnetic resonance imaging contrast agents in human serum at 37°C, Investig. Radiol. 43 (2008) 817, https://doi.org/10.1097/RLI.0b013e3181852171.

[8] A. Bianchi, L. Calabi, F. Corana, S. Fontana, P. Losi, A. Maiocchi, L. Paleari, B. Valtancoli, Thermodynamic and structural properties of Gd(III) complexes with polyamino-polycarboxylic ligands: basic compounds for the development of MRI contrast agents, Coord. Chem. Rev. 204 (2000) 309–393, https://doi.org/10.1016/S0010-8545(99)00237-4.

[9] E. Lancelot, J.-S. Raynaud, P. Desché, Current and future MR contrast agents: seeking a better chemical stability and relaxivity for optimal safety and efficacy, Investig. Radiol. 55 (2020) 578, https://doi.org/10.1097/RLI.0000000000000684.

[10] Q.N. Do, R.E. Lenkinski, G. Tircso, Z. Kovacs, How the chemical properties of GBCAs influence their safety profiles in vivo, Molecules 27 (2022) 58, https://doi.org/10.3390/molecules27010058.

[11] J. Vymazal, A.M. Rulseh, MRI contrast agents and retention in the brain: review of contemporary knowledge and recommendations to the future, Insights Imaging 15 (2024) 179, https://doi.org/10.1186/s13244-024-01763-z.

[12] A.J. van der Molen, C.C. Quattrocchi, C.A. Mallio, I.A. Dekkers, B.G.R. for the European Society of Magnetic Resonance in Medicine Educational Committee (ESMRMB-GREC), Ten years of gadolinium retention and deposition: ESMRMB-GREC looks backward and forward, Eur. Radiol. 34 (2024) 600–611, https://doi.org/10.1007/s00330-023-10281-3.

[13] M. Botta, Second coordination sphere water molecules and relaxivity of Gadolinium(III) complexes: implications for MRI contrast agents, Eur. J. Inorg. Chem. 2000 (2000) 399–407, https://doi.org/10.1002/(SICI)1099-0682(200003)2000:3<399::AID-EJIC399>3.0.CO;2-B.

[14] I. Solomon, Relaxation processes in a System of two spins, Phys. Rev. 99 (1955) 559–565, https://doi.org/10.1103/PhysRev.99.559.

[15] N. Bloembergen, Proton relaxation times in paramagnetic solutions, J. Chem. Phys. 27 (1957) 572–573.

[16] N. Bloembergen, L.O. Morgan, Proton relaxation times in paramagnetic solutions. Effects of electron spin relaxation, J. Chem. Phys. 34 (1961) 842–850, https://doi.org/10.1063/1.1731684.

[17] P. Caravan, J.J. Ellison, T.J. McMurry, R.B. Lauffer, Gadolinium(III) chelates as MRI contrast agents: structure, dynamics, and applications, Chem. Rev. 99 (1999) 2293–2352, https://doi.org/10.1021/cr980440x.

[18] G.M. Nicolle, É. Tóth, H. Schmitt-Willich, B. Radüchel, A.E. Merbach, The impact of rigidity and water exchange on the relaxivity of a dendritic MRI contrast agent, Chem. Eur J. 8 (2002) 1040–1048, https://doi.org/10.1002/1521-3765(20020301)8:5<1040::AID-CHEM1040>3.0.CO;2-D.

[19] É. Tóth, L. Helm, K.E. Kellar, A.E. Merbach, Gd(DTPA-bisamide)alkyl copolymers: a hint for the Formation of MRI contrast agents with very high relaxivity, Chem. Eur J. 5 (1999) 1202–1211, https://doi.org/10.1002/(SICI)1521-3765(19990401)5:4<1202::AID-CHEM1202>3.0.CO;2-Y.

[20] G.M. Nicolle, É. Tóth, K.-P. Eisenwiener, H.R. Mäcke, A.E. Merbach, From monomers to micelles: investigation of the parameters influencing proton relaxivity, JBIC, J. Biol. Inorg. Chem. 7 (2002) 757–769, https://doi.org/10.1007/s00775-002-0353-3.

[21] C. Robic, M. Port, O. Rousseaux, S. Louguet, N. Fretellier, S. Catoen, C. Factor, S. Le Greneur, C. Medina, P. Bourrinet, I. Raynal, J.-M. Idée, C. Corot, Physicochemical and pharmacokinetic profiles of gadopiclenol, Investig. Radiol. 54 (2019) 475–484, https://doi.org/10.1097/RLI.0000000000000563.

[22] J. Lohrke, M. Berger, T. Frenzel, C.-S. Hilger, G. Jost, O. Panknin, M. Bauser, W. Ebert, H. Pietsch, Preclinical profile of gadoquatrane: a novel tetrameric, macrocyclic high relaxivity gadolinium-based contrast agent, Investig. Radiol. 57 (2022) 629, https://doi.org/10.1097/RLI.0000000000000889.

[23] M. Rohrer, H. Bauer, J. Mintorovitch, M. Requardt, H.-J. Weinmann, Comparison of magnetic properties of MRI contrast media solutions at different magnetic field strengths, Investig. Radiol. 40 (2005) 715, https://doi.org/10.1097/01.rli.0000184756.66360.d3.

[24] I. Maimouni, C. Henoumont, M.-C. De Goltstein, J.-F. Mayer, A. Dehimi, Y. Boubeguira, C. Kattenbeck, T.J. Maas, N. Decout, I. Strzeminska, G. Bazin, C. Medina, C. Factor, O. Rousseaux, U. Karst, S. Laurent, S. Catoen, Gadopiclenol: a q = 2 Gadolinium-Based MRI contrast agent combining high stability and efficacy, Investig. Radiol. 60 (2025) 234, https://doi.org/10.1097/RLI.0000000000001121.

[25] K. Peldschus, M. Hamdorf, P. Robert, M. Port, J. Graessner, G. Adam, C. U. Herborn, Contrast-Enhanced magnetic resonance angiography: evaluation of the high relaxivity low diffusible gadolinium-based contrast agent P846 in comparison with gadoterate meglumine in rabbits at 1.5 tesla and 3.0 tesla, Investig. Radiol. 43 (2008) 837, https://doi.org/10.1097/RLI.0b013e3181852158.

[26] M. Port, C. Corot, I. Raynal, J.-M. Idee, A. Dencausse, E. Lancelot, D. Meyer, B. Bonnemain, J. Lautrou, Physicochemical and biological evaluation of P792, a rapid-clearance blood-pool agent for magnetic resonance imaging, Investig. Radiol. 36 (2001) 445.

[27] P. Caravan, C.T. Farrar, L. Frullano, R. Uppal, Influence of molecular parameters and increasing magnetic field strength on relaxivity of gadolinium- and manganese-based T1 contrast agents, Contrast Media Mol. Imaging 4 (2009) 89–100, https://doi.org/10.1002/cmmi.267.

[28] K. Overoye-Chan, S. Koerner, R.J. Looby, A.F. Kolodziej, S.G. Zech, Q. Deng, J. M. Chasse, T.J. McMurry, P. Caravan, EP-2104R: a fibrin-specific gadolinium-based MRI contrast agent for detection of thrombus, J. Am. Chem. Soc. 130 (2008) 6025–6039, https://doi.org/10.1021/ja800834y.

[29] M. Port, C. Corot, X. Violas, P. Robert, I. Raynal, G. Gagneur, How to compare the efficiency of albumin-bound and Nonalbumin-Bound contrast agents in vivo: the concept of dynamic relaxivity, Investig. Radiol. 40 (2005) 565, https://doi.org/10.1097/01.rli.0000175388.98721.9b.

[30] L.V. Elst, F. Maton, S. Laurent, F. Seghi, F. Chapelle, R.N. Muller, A multinuclear MR study of Gd-EOB-DTPA: comprehensive preclinical characterization of an organ specific MRI contrast agent, Magn. Reson. Med. 38 (1997) 604–614, https://doi.org/10.1002/mrm.1910380415.

[31] P. Caravan, N.J. Cloutier, M.T. Greenfield, S.A. McDermid, S.U. Dunham, J.W. M. Bulte, John C. Amedio, R.J. Looby, R.M. Supkowski, William DeW. Horrocks, T.J. McMurry, R.B. Lauffer, The interaction of MS-325 with human serum albumin and its effect on proton relaxation rates, J. Am. Chem. Soc. 124 (2002) 3152–3162, https://doi.org/10.1021/ja017168k.

[32] M. Goyen, Gadofosveset-enhanced magnetic resonance angiography, Vasc, Healthc. Risk Manag. 4 (2008) 1–9, https://doi.org/10.2147/vhrm.s411.

[33] S. Aime, M. Botta, M. Fasano, S.G. Crich, E. Terreno, Gd(III) complexes as contrast agents for magnetic resonance imaging: a proton relaxation enhancement study of the interaction with human serum albumin, JBIC, J. Biol. Inorg. Chem. 1 (1996) 312–319, https://doi.org/10.1007/s007750050059.

[34] P. Urbanovský, J. Kotek, F. Carniato, M. Botta, P. Hermann, Lanthanide complexes of DO3A–(Dibenzylamino)methylphosphinate: effect of Protonation of the Dibenzylamino Group on the water-exchange rate and the binding of human serum albumin, Inorg. Chem. 58 (2019) 5196–5210, https://doi.org/10.1021/acs.inorgchem.9b00267.

[35] D.L. Longo, F. Arena, L. Consolino, P. Minazzi, S. Geninatti-Crich, G. B. Giovenzana, S. Aime, Gd-AAZTA-MADEC, an improved blood pool agent for DCE-MRI studies on mice on 1 T scanners, Biomaterials 75 (2016) 47–57, https://doi.org/10.1016/j.biomaterials.2015.10.012.

[36] M. Woods, Z. Kovacs, S. Zhang, A.D. Sherry, Towards the rational design of magnetic resonance imaging contrast agents: isolation of the two coordination isomers of lanthanide DOTA-Type complexes, Angew. Chem. Int. Ed. 42 (2003) 5889–5892, https://doi.org/10.1002/anie.200352234.

[37] S. Aime, A. Barge, M. Botta, A.S. De Sousa, D. Parker, Direct NMR spectroscopic observation of a lanthanide-coordinated water molecule whose exchange rate is dependent on the conformation of the complexes, Angew. Chem. Int. Ed. 37 (1998) 2673–2675.

[38] S. Aime, M. Botta, Z. Garda, B.E. Kucera, G. Tircso, V.G. Young, M. Woods, Properties, solution State behavior, and crystal structures of chelates of DOTMA, Inorg. Chem. 50 (2011) 7955–7965, https://doi.org/10.1021/ic2012827.

[39] K.B. Maier, L.N. Rust, F. Carniato, M. Botta, M. Woods, α-Aryl substituted GdDOTA derivatives, the perfect contrast agents for MRI? Chem. Commun. 60 (2024) 2898–2901, https://doi.org/10.1039/D3CC05989H.

[40] L.R. Tear, C. Carrera, E. Gianolio, S. Aime, Towards an improved design of MRI contrast agents: synthesis and relaxometric characterisation of Gd-HPDO3A analogues, Chem. Eur J. 26 (2020) 6056–6063, https://doi.org/10.1002/chem.202000479.

[41] L.R. Tear, C. Carrera, C.B. Dhakan, E. Cavallari, F. Travagin, C. Calcagno, S. Aime, E. Gianolio, An albumin-binding Gd-HPDO3A contrast agent for improved intravascular retention, Inorg. Chem. Front. 8 (2021) 4014–4025, https://doi.org/10.1039/D1QI00128K.

[42] F. Hasallari, C. Carrera, E. Cavallari, E. Gianolio, S. Aime, A novel albumin-binding macrocyclic Gd-HPDO3A complex bearing a deoxycholic acid residue: the role of the hydration state, water exchange and local dynamics in the observed relaxivity, Inorg. Chem. Front. 11 (2024) 6511–6526, https://doi.org/10.1039/D4QI00894D.

[43] G. Lipari, A. Szabo, Model-free approach to the interpretation of nuclear magnetic resonance relaxation in macromolecules. 1. Theory and range of validity, J. Am. Chem. Soc. 104 (1982) 4546–4559, https://doi.org/10.1021/ja00381a009.

[44] P. Caravan, Strategies for increasing the sensitivity of gadolinium based MRI contrast agents, Chem. Soc. Rev. 35 (2006) 512–523, https://doi.org/10.1039/B510982P.

[45] S. Avedano, L. Tei, A. Lombardi, G.B. Giovenzana, S. Aime, D. Longo, M. Botta, Maximizing the relaxivity of HSA-bound gadolinium complexes by simultaneous optimization of rotation and water exchange, Chem. Commun. (2007) 4726–4728, https://doi.org/10.1039/B714438E.

[46] M. Botta, S. Avedano, G.B. Giovenzana, A. Lombardi, D. Longo, C. Cassino, L. Tei, S. Aime, Relaxometric Study of a series of monoaqua GdIII complexes of rigidified EGTA-Like chelators and their noncovalent interaction with human serum albumin, Eur. J. Inorg. Chem. 2011 (2011) 802–810, https://doi.org/10.1002/ejic.201001103.

[47] R. Ruloff, É. Tóth, R. Scopelliti, R. Tripier, H. Handel, A.E. Merbach, Accelerating water exchange for GdIII chelates by steric compression around the water binding site, Chem. Commun. (2002) 2630–2631, https://doi.org/10.1039/B207713B.

[48] S. Laus, R. Ruloff, É. Tóth, A.E. Merbach, GdIII complexes with fast water exchange and high thermodynamic stability: potential building blocks for high-relaxivity MRI contrast agents, Chem. Eur J. 9 (2003) 3555–3566, https://doi.org/10.1002/chem.200204612.

[49] J. Yu, A.F. Martins, C. Preihs, V. Clavijo Jordan, S. Chirayil, P. Zhao, Y. Wu, K. Nasr, G.E. Kiefer, A.D. Sherry, Amplifying the sensitivity of Zinc(II) responsive MRI contrast agents by altering water exchange rates, J. Am. Chem. Soc. 137 (2015) 14173–14179, https://doi.org/10.1021/jacs.5b09158.

[50] E. Gianolio, G.B. Giovenzana, D. Longo, I. Longo, I. Menegotto, S. Aime, Relaxometric and modelling studies of the binding of a lipophilic Gd-AAZTA complex to fatted and defatted human serum albumin, Chem. Eur J. 13 (2007) 5785–5797, https://doi.org/10.1002/chem.200601277.

[51] R. Stefania, L. Palagi, E. Di Gregorio, G. Ferrauto, V. Dinatale, S. Aime, E. Gianolio, Seeking for innovation with magnetic resonance imaging paramagnetic contrast agents: relaxation enhancement via weak and dynamic electrostatic interactions with positively charged groups on endogenous macromolecules, J. Am. Chem. Soc. 146 (2024) 134–144, https://doi.org/10.1021/jacs.3c06275.
[52] D. Li, M. Kirberger, J. Qiao, Z. Gui, S. Xue, F. Pu, J. Jiang, Y. Xu, S. Tan, M. Salarian, O. Ibhagui, K. Hekmatyar, J.J. Yang, Protein MRI contrast agents as an effective approach for precision molecular imaging, Investig. Radiol. 59 (2024) 170, https://doi.org/10.1097/RLI.0000000000001057.
[53] S. Aime, L. Frullano, S. Geninatti Crich, Compartmentalization of a gadolinium complex in the apoferritin cavity: a route to obtain high relaxivity contrast agents for magnetic resonance imaging, Angew. Chem. Int. Ed. 41 (2002) 1017–1019, https://doi.org/10.1002/1521-3773(20020315)41:6<1017::AID-ANIE1017>3.0.CO;2-P.
[54] J. Zhang, C. Yuan, L. Kong, F. Zhu, W. Yuan, J. Zhang, J. Hong, F. Deng, Q. Chen, C. Chen, T. Wang, Z. Zuo, M. Liang, H-ferritin-nanocaged gadolinium nanoparticles for ultra-sensitive MR molecular imaging, Theranostics 14 (2024) 1956–1965, https://doi.org/10.7150/thno.93856.
[55] R.B. Lauffer, T.J. Brady, Preparation and water relaxation properties of proteins labeled with paramagnetic metal chelates, Magn. Reson. Imaging 3 (1985) 11–16, https://doi.org/10.1016/0730-725X(85)90004-9.
[56] L.S. Karfeld, S.R. Bull, N.E. Davis, T.J. Meade, A.E. Barron, Use of a genetically engineered protein for the design of a multivalent MRI contrast agent, Bioconjug. Chem. 18 (2007) 1697–1700, https://doi.org/10.1021/bc700149u.
[57] G. Licciardi, D. Rizzo, M. Salobehaj, L. Massai, A. Geri, L. Messori, E. Ravera, M. Fragai, G. Parigi, Large protein assemblies for high-relaxivity contrast agents: the case of gadolinium-labeled asparaginase, Bioconjug. Chem. 33 (2022) 2411–2419, https://doi.org/10.1021/acs.bioconjchem.2c00506.
[58] J.J. Yang, J. Yang, L. Wei, O. Zurkiya, W. Yang, S. Li, J. Zou, Y. Zhou, A.L. W. Maniccia, H. Mao, F. Zhao, R. Malchow, S. Zhao, J. Johnson, X. Hu, E. Krogstad, Z.-R. Liu, Rational design of protein-based MRI contrast agents, J. Am. Chem. Soc. 130 (2008) 9260–9267, https://doi.org/10.1021/ja800736h.
[59] S. Xue, H. Yang, J. Qiao, F. Pu, J. Jiang, K. Hubbard, K. Hekmatyar, J. Langley, M. Salarian, R.C. Long, R.G. Bryant, X.P. Hu, H.E. Grossniklaus, Z.-R. Liu, J. J. Yang, Protein MRI contrast agent with unprecedented metal selectivity and sensitivity for liver cancer imaging, Proc. Natl. Acad. Sci. 112 (2015) 6607–6612, https://doi.org/10.1073/pnas.1423021112.
[60] S. Tan, H. Yang, S. Xue, J. Qiao, M. Salarian, K. Hekmatyar, Y. Meng, R. Mukkavilli, F. Pu, O.Y. Odubade, W. Harris, Y. Hai, M.L. Yushak, V.M. Morales-Tirado, P. Mittal, P.Z. Sun, D. Lawson, H.E. Grossniklaus, J.J. Yang, Chemokine receptor 4 targeted protein MRI contrast agent for early detection of liver metastases, Sci. Adv. 6 (2020) eaav7504, https://doi.org/10.1126/sciadv.aav7504.
[61] M. Salarian, R.C. Turaga, S. Xue, M. Nezafati, K. Hekmatyar, J. Qiao, Y. Zhang, S. Tan, O.Y. Ibhagui, Y. Hai, J. Li, R. Mukkavilli, M. Sharma, P. Mittal, X. Min, S. Keilholz, L. Yu, G. Qin, A.B. Farris, Z.-R. Liu, J.J. Yang, Early detection and staging of chronic liver diseases with a protein MRI contrast agent, Nat. Commun. 10 (2019) 4777, https://doi.org/10.1038/s41467-019-11984-2.
[62] O.Y. Ibhagui, D. Li, H. Han, G. Peng, M.L. Meister, Z. Gui, J. Qiao, M. Salarian, B. Dong, Y. Yuan, Y. Xu, H. Yang, S. Tan, G. Satyanarayana, S. Xue, R.C. Turaga, M. Sharma, Y. Hai, Y. Meng, K. Hekmatyar, P. Sun, G. Sica, X. Ji, Z. Liu, J.J. Yang, Early detection and staging of lung fibrosis enabled by collagen-targeted MRI protein contrast agent, Chem. Biomed. Imaging 1 (2023) 268–285, https://doi.org/10.1021/cbmi.3c00023.
[63] F. Pu, M. Salarian, S. Xue, J. Qiao, J. Feng, S. Tan, A. Patel, X. Li, K. Mamouni, K. Hekmatyar, J. Zou, D. Wu, J.J. Yang, Prostate-specific membrane antigen targeted protein contrast agents for molecular imaging of prostate cancer by MRI, Nanoscale 8 (2016) 12668–12682, https://doi.org/10.1039/C5NR09071G.
[64] J. Qiao, S. Li, L. Wei, J. Jiang, R. Long, H. Mao, L. Wei, L. Wang, H. Yang, H. E. Grossniklaus, Z.-R. Liu, J.J. Yang, HER2 Targeted Molecular MR Imaging Using a De Novo Designed Protein Contrast Agent, PLoS One 6 (2011) e18103, https://doi.org/10.1371/journal.pone.0018103.
[65] F. Carniato, L. Tei, A. Arrais, L. Marchese, M. Botta, Selective anchoring of GdIII chelates on the external surface of organo-modified mesoporous Silica nanoparticles: a new chemical strategy to enhance relaxivity, Chem. Eur J. 19 (2013) 1421–1428, https://doi.org/10.1002/chem.201202670.
[66] B. Sitharaman, K.R. Kissell, K.B. Hartman, L.A. Tran, A. Baikalov, I. Rusakova, Y. Sun, H.A. Khant, S.J. Ludtke, W. Chiu, S. Laus, É. Tóth, L. Helm, A.E. Merbach, L.J. Wilson, Superparamagnetic gadonanotubes are high-performance MRI contrast agents, Chem. Commun. (2005) 3915–3917, https://doi.org/10.1039/B504435A.
[67] M.W. Rotz, K.S.B. Culver, G. Parigi, K.W. MacRenaris, C. Luchinat, T.W. Odom, T. J. Meade, High relaxivity Gd(III)–DNA gold nanostars: investigation of shape effects on proton relaxation, ACS Nano 9 (2015) 3385–3396, https://doi.org/10.1021/nn5070953.
[68] P. Fatehbasharzad, R. Stefania, C. Carrera, I. Hawala, D. Delli Castelli, S. Baroni, M. Colombo, D. Prosperi, S. Aime, Relaxometric studies of Gd-Chelate conjugated on the surface of differently shaped gold nanoparticles, Nanomaterials 10 (2020) 1115, https://doi.org/10.3390/nano10061115.
[69] F. Carniato, L. Tei, M. Botta, Gd-Based mesoporous silica nanoparticles as MRI probes, Eur. J. Inorg. Chem. 2018 (2018) 4936–4954, https://doi.org/10.1002/ejic.201801039.
[70] F. Carniato, L. Tei, W. Dastrù, L. Marchese, M. Botta, Relaxivity modulation in Gd-functionalised mesoporous silicas, Chem. Commun. (2009) 1246–1248, https://doi.org/10.1039/B820591D.
[71] A.K. Duncan, P.J. Klemm, K.N. Raymond, C.C. Landry, Silica microparticles as a solid support for gadolinium phosphonate magnetic resonance imaging contrast agents, J. Am. Chem. Soc. 134 (2012) 8046–8049, https://doi.org/10.1021/ja302183w.
[72] F. Carniato, L. Tei, M. Cossi, L. Marchese, M. Botta, A chemical strategy for the relaxivity enhancement of GdIII chelates anchored on mesoporous Silica nanoparticles, Chem. Eur J. 16 (2010) 10727–10734, https://doi.org/10.1002/chem.201000499.
[73] D. Yuan, C.M. Ellis, F.E. Mózes, J.J. Davis, Ultrahigh magnetic resonance contrast switching with water gated polymer–silica nanoparticles, Chem. Commun. 59 (2023) 6008–6011, https://doi.org/10.1039/D3CC01205K.
[74] N. Wartenberg, P. Fries, O. Raccurt, A. Guillermo, D. Imbert, M. Mazzanti, A gadolinium complex confined in Silica nanoparticles as a highly efficient T1/T2 MRI contrast agent, Chem. Eur J. 19 (2013) 6980–6983, https://doi.org/10.1002/chem.201300635.
[75] S. Garifo, T. Vangijzegem, D. Stanicki, S. Laurent, A review on the design of carbon-based nanomaterials as MRI contrast agents, Molecules 29 (2024) 1639, https://doi.org/10.3390/molecules29071639.
[76] A. Rodríguez-Galván, M. Rivera, P. García-López, L.A. Medina, V.A. Basiuk, Gadolinium-containing carbon nanomaterials for magnetic resonance imaging: trends and challenges, J. Cell Mol. Med. 24 (2020) 3779–3794, https://doi.org/10.1111/jcmm.15065.
[77] L.M. Manus, D.J. Mastarone, E.A. Waters, X.-Q. Zhang, E.A. Schultz-Sikma, K. W. MacRenaris, D. Ho, T.J. Meade, Gd(III)-Nanodiamond conjugates for MRI contrast enhancement, Nano Lett. 10 (2010) 484–489, https://doi.org/10.1021/nl903264h.
[78] A.M. Panich, M. Salti, S.D. Goren, E.B. Yudina, A.E. Aleksenskii, A.Y. Vul', A. I. Shames, Gd(III)-Grafted detonation nanodiamonds for MRI contrast enhancement, J. Phys. Chem. C 123 (2019) 2627–2631, https://doi.org/10.1021/acs.jpcc.8b11655.
[79] B. Sitharaman, M. Van Der Zande, J.S. Ananta, X. Shi, A. Veltien, X. F. Walboomers, L.J. Wilson, A.G. Mikos, A. Heerschap, J.A. Jansen, Magnetic resonance imaging studies on gadonanotube-reinforced biodegradable polymer nanocomposites, J. Biomed. Mater. Res. 93A (2010) 1454–1462, https://doi.org/10.1002/jbm.a.32650.
[80] L. Wang, X. Zhu, X. Tang, C. Wu, Z. Zhou, C. Sun, S.-L. Deng, H. Ai, J. Gao, A multiple gadolinium complex decorated fullerene as a highly sensitive T1 contrast agent, Chem. Commun. 51 (2015) 4390–4393, https://doi.org/10.1039/C5CC00285K.
[81] J. Zhang, P.P. Fatouros, C. Shu, J. Reid, L.S. Owens, T. Cai, H.W. Gibson, G. L. Long, F.D. Corwin, Z.-J. Chen, H.C. Dorn, High relaxivity trimetallic Nitride (Gd3N) metallofullerene MRI contrast agents with optimized functionality, Bioconjug. Chem. 21 (2010) 610–615, https://doi.org/10.1021/bc900375n.
[82] A.H. Hung, M.C. Duch, G. Parigi, M.W. Rotz, L.M. Manus, D.J. Mastarone, K. T. Dam, C.C. Gits, K.W. MacRenaris, C. Luchinat, M.C. Hersam, T.J. Meade, Mechanisms of Gadographene-Mediated proton spin relaxation, J. Phys. Chem. C 117 (2013) 16263–16273, https://doi.org/10.1021/jp406909b.
[83] K.B. Hartman, S. Laus, R.D. Bolskar, R. Muthupillai, L. Helm, E. Toth, A. E. Merbach, L.J. Wilson, Gadonanotubes as ultrasensitive pH-Smart probes for magnetic resonance imaging, Nano Lett. 8 (2008) 415–419, https://doi.org/10.1021/nl0720408.
[84] M. Ricci, F. Carniato, L. Tei, S. Camorali, G. Ferrauto, M. Botta, Chitosan-Based nanogels containing Ln3+ chelates (Ln=Gd, Dy) as T1 and T2 MRI probes, Eur. J. Inorg. Chem. 27 (2024) e202300675, https://doi.org/10.1002/ejic.202300675.
[85] M. Callewaert, V.G. Roullin, C. Cadiou, E. Millart, L.V. Gulik, M.C. Andry, C. Portefaix, C. Hoeffel, S. Laurent, L.V. Elst, R. Muller, M. Molinari, F. Chuburu, Tuning the composition of biocompatible Gd nanohydrogels to achieve hypersensitive dual T1/T2 MRI contrast agents, J. Mater. Chem. B 2 (2014) 6397–6405, https://doi.org/10.1039/C4TB00783B.
[86] F. Carniato, L. Tei, M. Botta, E. Ravera, M. Fragai, G. Parigi, C. Luchinat, 1H NMR relaxometric study of chitosan-based nanogels containing Mono- and bis-hydrated Gd(III) chelates: clues for MRI probes of improved sensitivity, ACS Appl. Bio Mater. 3 (2020) 9065–9072, https://doi.org/10.1021/acsabm.0c01295.
[87] F. Carniato, M. Ricci, L. Tei, F. Garello, E. Terreno, E. Ravera, G. Parigi, C. Luchinat, M. Botta, High relaxivity with no coordinated waters: a seemingly paradoxical behavior of [Gd(DOTP)]5– embedded in nanogels, Inorg. Chem. 61 (2022) 5380–5387, https://doi.org/10.1021/acs.inorgchem.2c00225.
[88] E. Rosa, F. Carniato, L. Tei, C. Diaferia, G. Morelli, M. Botta, A. Accardo, Peptide-Based hydrogels and nanogels containing Gd(III) complexes as T1 relaxation agents, Pharmaceuticals 15 (2022) 1572, https://doi.org/10.3390/ph15121572.
[89] S. Avedano, M. Botta, J.S. Haigh, D.L. Longo, M. Woods, Coupling fast water exchange to slow molecular tumbling in Gd3+ chelates: why faster is not always better, Inorg. Chem. 52 (2013) 8436–8450, https://doi.org/10.1021/ic400308a.
[90] M.P. Lowe, D. Parker, O. Reany, S. Aime, M. Botta, G. Castellano, E. Gianolio, R. Pagliarin, pH-Dependent modulation of relaxivity and luminescence in macrocyclic gadolinium and Europium complexes based on reversible intramolecular sulfonamide ligation, J. Am. Chem. Soc. 123 (2001) 7601–7609, https://doi.org/10.1021/ja0103647.
[91] E. Terreno, M. Botta, P. Boniforte, C. Bracco, L. Milone, B. Mondino, F. Uggeri, S. Aime, A multinuclear NMR relaxometry Study of ternary adducts formed between heptadentate GdIII chelates and L-Lactate, Chem. Eur J. 11 (2005) 5531–5537, https://doi.org/10.1002/chem.200500129.
[92] S. Aime, E. Gianolio, E. Terreno, G.B. Giovenzana, R. Pagliarin, M. Sisti, G. Palmisano, M. Botta, M.P. Lowe, D. Parker, Ternary Gd(III)L-HSA adducts: evidence for the replacement of inner-sphere water molecules by coordinating

groups of the protein. Implications for the design of contrast agents for MRI, JBIC, J. Biol. Inorg. Chem. 5 (2000) 488–497, https://doi.org/10.1007/PL00021449.
[93] S. Aime, M. Botta, S. Geninatti Crich, G.B. Giovenzana, G. Jommi, R. Pagliarin, M. Sisti, Synthesis and NMR studies of three pyridine-containing triaza macrocyclic triacetate ligands and their complexes with lanthanide ions, Inorg. Chem. 36 (1997) 2992–3000, https://doi.org/10.1021/ic960794b.
[94] S.M. Cohen, J. Xu, E. Radkov, K.N. Raymond, M. Botta, A. Barge, S. Aime, Syntheses and relaxation properties of mixed gadolinium hydroxypyridinonate MRI contrast agents, Inorg. Chem. 39 (2000) 5747–5756, https://doi.org/10.1021/ic000563b.
[95] S. Aime, L. Calabi, C. Cavallotti, E. Gianolio, G.B. Giovenzana, P. Losi, A. Maiocchi, G. Palmisano, M. Sisti, [Gd-AAZTA]-: a new structural entry for an improved generation of MRI contrast agents, Inorg. Chem. 43 (2004) 7588–7590, https://doi.org/10.1021/ic0489692.
[96] L. Pellegatti, J. Zhang, B. Drahos, S. Villette, F. Suzenet, G. Guillaumet, S. Petoud, É. Tóth, Pyridine-based lanthanidecomplexes: towards bimodal agents operating as near infrared luminescent and MRI reporters, Chem. Commun. (2008) 6591–6593, https://doi.org/10.1039/B817343E.
[97] L. Leone, L. Guarnieri, J. Martinelli, M. Sisti, A. Penoni, M. Botta, L. Tei, Rigid and compact Binuclear bis-hydrated Gd-complexes as high relaxivity MRI agents, Chem. Eur J. 27 (2021) 11811–11817, https://doi.org/10.1002/chem.202101701.
[98] F.V.C. Kock, A. Forgács, N. Guidolin, R. Stefania, A. Vágner, E. Gianolio, S. Aime, Z. Baranyai, [Gd(AAZTA)]− derivatives with n-Alkyl acid side chains show improved properties for their application as MRI contrast agents, Chem. Eur J. 27 (2021) 1849–1859, https://doi.org/10.1002/chem.202004479.
[99] S. Chaves, K. Gwizdała, K. Chand, L. Gano, A. Pallier, É. Tóth, M.A. Santos, GdIII and GaIII complexes with a new tris-3,4-HOPO ligand as new imaging probes: complex stability, magnetic properties and biodistribution, Dalton Trans. 51 (2022) 6436–6447, https://doi.org/10.1039/D2DT00066K.
[100] Y. Jian, G. Mo, W. Xu, Y. Liu, Z. Zhang, Y. Ding, R. Gao, J. Xu, J. Zhu, K. Shu, Z. Yan, F. Carniato, C. Platas-Iglesias, F. Ye, M. Botta, L. Dai, Chiral pyclen-based heptadentate chelates as highly stable MRI contrast agents, Inorg. Chem. 63 (2024) 8462–8475, https://doi.org/10.1021/acs.inorgchem.4c01028.
[101] O. Porcar-Tost, J.A. Olivares, A. Pallier, D. Esteban-Gómez, O. Illa, C. Platas-Iglesias, É. Tóth, R.M. Ortuño, Gadolinium complexes of highly rigid, open-chain ligands containing a cyclobutane ring in the backbone: decreasing ligand denticity might enhance kinetic inertness, Inorg. Chem. 58 (2019) 13170–13183, https://doi.org/10.1021/acs.inorgchem.9b02044.
[102] B. Zhang, L. Cheng, B. Duan, W. Tang, Y. Yuan, Y. Ding, A. Hu, Gadolinium complexes of diethylenetriamine-N-oxide pentaacetic acid-bisamide: a new class of highly stable MRI contrast agents with a hydration number of 3, Dalton Trans. 48 (2019) 1693–1699, https://doi.org/10.1039/C8DT04478C.
[103] M. Khannam, S.K. Sahoo, C. Mukherjee, Effect of ligand chirality and hyperconjugation on the thermodynamic stability of a Tris(aquated) GdIII complex: synthesis, characterization, and T1-Weighted phantom MR image study, Eur. J. Inorg. Chem. 2019 (2019) 2518–2523, https://doi.org/10.1002/ejic.201900043.
[104] S. Aime, M. Botta, D. Parker, J.A.G. Williams, Extent of hydration of octadentate lanthanide complexes incorporating phosphinate donors: solution relaxometry and luminescence studies, J. Chem. Soc. Dalton Trans. (1996) 17–23, https://doi.org/10.1039/DT9960000017.
[105] S. Aime, M. Botta, E. Terreno, P.L. Anelli, F. Uggeri, Gd(DOTP)5- outer-sphere relaxation enhancement promoted by nitrogen bases, Magn. Reson. Med. 30 (1993) 583–591, https://doi.org/10.1002/mrm.1910300509.
[106] P. Lebdušková, P. Hermann, L. Helm, É. Tóth, J. Kotek, K. Binnemans, J. Rudovský, I. Lukeš, A.E. Merbach, Gadolinium(III) complexes of mono- and diethyl esters of monophosphonic acid analogue of DOTA as potential MRI contrast agents: solution structures and relaxometric studies, Dalton Trans. (2007) 493–501, https://doi.org/10.1039/B612876A.
[107] V. Jacques, S. Dumas, W.-C. Sun, J.S. Troughton, M.T. Greenfield, P. Caravan, High-Relaxivity magnetic resonance imaging contrast agents part 2: optimization of Inner- and second-sphere relaxivity, Investig. Radiol. 45 (2010) 613–624, https://doi.org/10.1097/RLI.0b013e3181ee6a49.
[108] S. Camorali, L. Leone, L. Piscopo, L. Tei, Relaxivity modulation of Gd-HPDO3A-like complexes by introducing polar and protic peripheral groups, Molecules 29 (2024) 4663, https://doi.org/10.3390/molecules29194663.
[109] L. Lattuada, D. Horváth, S.C. Serra, A.F. Mingo, P. Minazzi, A. Bényei, A. Forgács, F. Fedeli, E. Gianolio, S. Aime, G.B. Giovenzana, Z. Baranyai, Enhanced relaxivity of Gd III -complexes with HP-DO3A-like ligands upon the activation of the intramolecular catalysis of the prototropic exchange, Inorg. Chem. Front. 8 (2021) 1500–1510, https://doi.org/10.1039/D0QI01333A.
[110] S. Aime, S. Baroni, D. Delli Castelli, E. Brücher, I. Fábián, S.C. Serra, A. Fringuello Mingo, R. Napolitano, L. Lattuada, F. Tedoldi, Z. Baranyai, Exploiting the proton exchange as an additional route to enhance the relaxivity of paramagnetic MRI contrast agents, Inorg. Chem. 57 (2018) 5567–5574, https://doi.org/10.1021/acs.inorgchem.8b00521.
[111] A. Fringuello Mingo, S. Colombo Serra, S. Baroni, C. Cabella, R. Napolitano, I. Hawala, I.M. Carnovale, L. Lattuada, F. Tedoldi, S. Aime, Macrocyclic paramagnetic agents for MRI: determinants of relaxivity and strategies for their improvement, Magn. Reson. Med. 78 (2017) 1523–1532, https://doi.org/10.1002/mrm.26519.
[112] I. Maria Carnovale, M. Lucio Lolli, S. Colombo Serra, A. Fringuello Mingo, R. Napolitano, V. Boi, N. Guidolin, L. Lattuada, F. Tedoldi, Z. Baranyai, S. Aime, Exploring the intramolecular catalysis of the proton exchange process to modulate the relaxivity of gd(iii)-complexes of HP-DO3A-like ligands, Chem. Commun. 54 (2018) 10056–10059, https://doi.org/10.1039/C8CC05284K.
[113] L. Leone, M. Boccalon, G. Ferrauto, I. Fábián, Z. Baranyai, L. Tei, Acid-catalyzed proton exchange as a novel approach for relaxivity enhancement in Gd-HPDO3A-like complexes, Chem. Sci. 11 (2020) 7829–7835, https://doi.org/10.1039/D0SC02174A.
[114] S. Trattnig, G. Hangel, S.D. Robinson, V. Juras, P. Szomolanyi, A. Dal-Bianco, Ultrahigh-field MRI: where it really makes a difference, Radiol. (2023), https://doi.org/10.1007/s00117-023-01184-x.
[115] D. Ivanov, F. De Martino, E. Formisano, F.J. Fritz, R. Goebel, L. Huber, S. Kashyap, V.G. Kemper, D. Kurban, A. Roebroeck, S. Sengupta, B. Sorger, D.H. Y. Tse, K. Uludağ, C.J. Wiggins, B.A. Poser, Magnetic resonance imaging at 9.4 T: the Maastricht journey, Magn. Reson. Mater. Phys. Biol. Med. 36 (2023) 159–173, https://doi.org/10.1007/s10334-023-01080-4.
[116] T. Vaughan, L. DelaBarre, C. Snyder, J. Tian, C. Akgun, D. Shrivastava, W. Liu, C. Olson, G. Adriany, J. Strupp, P. Andersen, A. Gopinath, P.-F. van de Moortele, M. Garwood, K. Ugurbil, 9.4T human MRI: preliminary results, Magn. Reson. Med. 56 (2006) 1274–1282, https://doi.org/10.1002/mrm.21073.
[117] N. Boulant, L. Quettier, G. Aubert, A. Amadon, J. Belorgey, C. Berriaud, C. Bonnelye, Ph Bredy, E. Chazel, G. Dilasser, O. Dubois, E. Giacomini, G. Gilgrass, V. Gras, Q. Guihard, V. Jannot, F.P. Juster, H. Lannou, F. Leprêtre, C. Lerman, C. Le Ster, M. Luong, F. Mauconduit, F. Molinié, F. Nunio, L. Scola, A. Sinanna, R. Touzery, P. Védrine, A. Vignaud, The Iseult Consortium, commissioning of the Iseult CEA 11.7 T whole-body MRI: current status, gradient–magnet interaction tests and first imaging experience, Magn. Reson. Mater. Phys. Biol. Med. 36 (2023) 175–189, https://doi.org/10.1007/s10334-023-01063-5.
[118] I.M. Noebauer-Huhmann, P. Szomolanyi, V. Juras, O. Kraff, M.E. Ladd, S. Trattnig, Gadolinium-based magnetic resonance contrast agents at 7 tesla: in vitro T: 1: relaxivities in human blood plasma, Investig. Radiol. 45 (2010) 554, https://doi.org/10.1097/RLI.0b013e3181ebd4e3.
[119] P. Fries, A. Massmann, P. Robert, C. Corot, M.W. Laschke, G. Schneider, A. Buecker, A. Müller, Evaluation of gadopiclenol and P846, 2 high-relaxivity macrocyclic magnetic resonance contrast agents without protein binding, in a rodent model of hepatic metastases: potential solutions for improved enhancement at ultrahigh field strength, Investig. Radiol. 54 (2019) 549, https://doi.org/10.1097/RLI.0000000000000572.
[120] J.B. Livramento, L. Helm, A. Sour, C. O'Neil, A.E. Merbach, É. Tóth, A benzene-core trinuclear GdIII complex: towards the optimization of relaxivity for MRI contrast agent applications at high magnetic field, Dalton Trans. (2008) 1195–1202, https://doi.org/10.1039/B717390C.
[121] J.B. Livramento, É. Tóth, A. Sour, A. Borel, A.E. Merbach, R. Ruloff, High relaxivity confined to a small molecular space: a metallostar-based, potential MRI contrast agent, Angew. Chem. Int. Ed. 44 (2005) 1480–1484, https://doi.org/10.1002/anie.200461875.
[122] J.b. Livramento, C. Weidensteiner, M.i. m. Prata, P.r. Allegrini, C.f. g. c. Geraldes, L. Helm, R. Kneuer, A.e. Merbach, A.c. Santos, P. Schmidt, É. Tóth, First in vivo MRI assessment of a self-assembled metallostar compound endowed with a remarkable high field relaxivity, Contrast Media Mol. Imaging 1 (2006) 30–39, https://doi.org/10.1002/cmmi.92.
[123] L. Tei, G. Gugliotta, D. Marchi, M. Cossi, S.G. Crich, M. Botta, Optimizing the relaxivity at high fields: systematic variation of the rotational dynamics in polynuclear Gd-complexes based on the AAZTA ligand, Inorg. Chem. Front. 8 (2021) 4806–4819, https://doi.org/10.1039/D1QI00904D.
[124] F. Lux, V.L. Tran, E. Thomas, S. Dufort, F. Rossetti, M. Martini, C. Truillet, T. Doussineau, G. Bort, F. Denat, F. Boschetti, G. Angelovski, A. Detappe, Y. Crémillieux, N. Mignet, B.-T. Doan, B. Larrat, S. Meriaux, E. Barbier, S. Roux, P. Fries, A. Müller, M.-C. Abadjian, C. Anderson, E. Canet-Soulas, P. Bouziotis, M. Barberi-Heyob, C. Frochot, C. Verry, J. Balosso, M. Evans, J. Sidi-Boumedine, M. Janier, K. Butterworth, S. McMahon, K. Prise, M.-T. Aloy, D. Ardail, C. Rodriguez-Lafrasse, E. Porcel, S. Lacombe, R. Berbeco, A. Allouch, J.-L. Perfettini, C. Chargari, E. Deutsch, G. Le Duc, O. Tillement, AGuIX® from bench to bedside—Transfer of an ultrasmall theranostic gadolinium-based nanoparticle to clinical medicine, Br. J. Radiol. 92 (2019) 20180365, https://doi.org/10.1259/bjr.20180365.
[125] P. Fries, D. Morr, A. Müller, F. Lux, O. Tillement, A. Massmann, R. Seidel, T. Schäfer, M.D. Menger, G. Schneider, A. Bücker, Evaluation of a Gadolinium-Based Nanoparticle (AGuIX) for Contrast-Enhanced MRI of the Liver in a Rat Model of Hepatic Colorectal Cancer Metastases at 9.4 Tesla, RöFo - Fortschritte Auf Dem Geb. Röntgenstrahlen Bildgeb, Verfahr. 187 (2015) 1108–1115, https://doi.org/10.1055/s-0035-1553500.
[126] D. Lawson, A. Barge, E. Terreno, D. Parker, S. Aime, M. Botta, Optimizing the high-field relaxivity by self-assembling of macrocyclic Gd(III) complexes, Dalton Trans. 44 (2015) 4910–4917, https://doi.org/10.1039/C4DT02971B.
[127] S. Aime, P. Caravan, Biodistribution of gadolinium-based contrast agents, including gadolinium deposition, J. Magn. Reson. Imag. 30 (2009) 1259–1267, https://doi.org/10.1002/jmri.21969.
[128] N. Hoshyar, Samantha Gray, Hongbin G. Han, Bao, The Effect of Nanoparticle Size on in Vivo Pharmacokinetics and Cellular Interaction, Nanomed, vol. 11, 2016, pp. 673–692, https://doi.org/10.2217/nnm.16.5.
[129] M. Longmire, Peter L.H. Choyke, Kobayashi, Clearance properties of nano-sized particles and molecules as imaging agents: considerations and caveats, Nanomed 3 (2008) 703–717, https://doi.org/10.2217/17435889.3.5.703.
[130] H. Kobayashi, B. Turkbey, R. Watanabe, P.L. Choyke, Cancer drug delivery: considerations in the rational design of nanosized bioconjugates, Bioconjug. Chem. 25 (2014) 2093–2100, https://doi.org/10.1021/bc500481x.

[131] J.S. Suk, Q. Xu, N. Kim, J. Hanes, L.M. Ensign, PEGylation as a strategy for improving nanoparticle-based drug and gene delivery, Adv. Drug Deliv. Rev. 99 (2016) 28–51, https://doi.org/10.1016/j.addr.2015.09.012.
[132] J. Liu, Z. Xiong, J. Zhang, C. Peng, B. Klajnert-Maculewicz, M. Shen, X. Shi, Zwitterionic Gadolinium(III)-Complexed dendrimer-entrapped gold nanoparticles for enhanced computed tomography/magnetic resonance imaging of lung cancer metastasis, ACS Appl. Mater. Interfaces 11 (2019) 15212–15221, https://doi.org/10.1021/acsami.8b21679.
[133] M.J. Ernsting, M. Murakami, A. Roy, S.-D. Li, Factors controlling the pharmacokinetics, biodistribution and intratumoral penetration of nanoparticles, J. Contr. Release 172 (2013) 782–794, https://doi.org/10.1016/j.jconrel.2013.09.013.